Generation of entropy in micro thermofluidic and thermochemical energy systems-A critical review

Mehrdad Torabi [a], Nader Karimi [*, b,c], Mohsen Torabi [*, b], G.P. Peterson [d], Carey J. Simonson [a]

[a] Department of Mechanical Engineering, University of Saskatchewan, 57 Campus Drive, Saskatoon, SK S7N 5A9, Canada

[b] James Watt School of Engineering, University of Glasgow, Glasgow G12 8QQ, United Kingdom

[c] School of Engineering and Materials Science, Queen Mary University of London, London E1 4NS, United Kingdom

[c] The George W. Woodruff School of Mechanical Engineering, Georgia Institute of Technology, Atlanta, GA 30332, USA

Abstract

Micro energy systems have progressed significantly over the last two decades, as has the utilization of micro thermofluidic and thermochemical systems. Several studies were conducted to analyze the thermophysical and chemical characteristics of these systems. In general, the large rates of heat and mass transfer typically encountered in these microsystems make them susceptible to significant irreversibilities and as a result, poor second-law performances. Although the understanding and modelling of entropy generation rate in microsystems is an inevitable part of their performance analyses, no reviews were found on the second law analysis, and more specifically on the entropy generation rate of micro thermal and thermochemical systems. To address this shortcoming, the current review explores the mechanisms of entropy generation rate in these micro energy systems and identifies the possible future avenues of research in this field. The existing literature on entropy generation rate in micro single and multiphase thermofluidic systems, with the inclusion of various effects such as magnetic and electric fields, nanoparticles and thermochemical reactions are reviewed in detail. The unexplored and less investigated areas such as second law analysis of micro porous systems using pore-scale modeling and entropy generation rate of airflow through microchannels with inserts are identified, and recommendations are made for future research.

Keywords: Micro thermofluidic systems; Micro thermochemical systems; Second Law analysis; Entropy generation rate.

* Corresponding authors.
E-mails: Torabi_mech@yahoo.com (M. Torabi), Nader.Karimi@glasgow.ac.uk (N. Karimi), Bud.Peterson@gatech.edu (G.P. Peterson).

Table of Contents

Nomenclature

asf	interfacial area per unit volume of porous media, m−1	ρ	fluid density, kg.m−3
cp	specific heat capacity, J.kg−1.K−1	v	specific volume, m3.kg−1
hi	enthalpy of ith species, kJ.kg−1	**subscripts**	
hsf	solid-to-fluid convection heat transfer coefficient, W.m−2.K−1	a	air
i	internal energy, J	b	bulk
J	diffusion flux	$cond$	conduction
k	thermal conductivity, W.m−1.K−1	$diff$	diffusion
m	mass flow rate, kg.s−1	ef	effective fluid characteristic
	pressure, Pa	es	effective solid characteristic
Q	heat generation rate, W	eff	effective
	Constant for ideal gases, J.kg. K−1	f	fluid
s	entropy, J.K−1	g	gas
$Sgen$	entropy generation rate, W.K−1	in	input
S'''	local entropy generation rate, W.K−1.m−3	i	ith species
t	time, s	mix	mixture
T	temperature, K	m	mean
	velocity, m.s−1	out	output
	axial coordinate, m	r	reaction, refrigerant
y	transverse coordinate, m	rad	radiation
Y	ith species mole, mol	s	solid
Greek symbols		tot	total
κ	porous media permeability, m2	vis	viscous
μ	dynamic viscosity, kg.m−1.s−1, chemical potential, J.kg−1	w	wall
	viscous dissipation function, kg.m−1.s−3		

1. Introduction

The fast-growing utilization of micro manufacturing techniques has had a significant and lasting impact on a number of scientific and engineering areas of research. Among these, thermal systems are, perhaps, the most significantly impacted by these advances. Miniaturization has taken place in various energy-related systems such as heat exchangers [1], combustion systems [2], micro reactors [3], micro coolers [4,5], and drug delivery and infusion systems [6]. The ever present desire to continue to reduce the size and power requirements of devices has brought with it some significant challenges with respect to the thermophysical characteristics of these systems [7,8]. In addition to being smaller in feature size, the larger surface-to-volume ratio provides more interactions between the surfaces and the flowing fluid(s) in the system [3]. For example, larger surface-to-volume ratio results in greater thermal interaction between surface and surroundings [9]. Similarly, increasing surface-to-volume ratio facilitates chemical reactions in microreactors, which benefit from greater heat and mass exchange features [10,11]. The increasingly importance in the development of miniaturized thermal systems has resulted in various investigations on first and second law performance of these microsystems. Researchers have already investigated these systems from first law perspective and to date some reviews have been published on such analyses [10,12]. The existing reviews cover temperature simulations [13] and visualizations [14], heat flux investigations and optimizations [15,16], and design study [17–19] in micro-size devices, i.e., devices with a length scale between 1 to 1000 micrometers. Yet, so far, there is no comprehensive review on the exergetic and entropy generation rate behaviors of these micro thermal and thermochemical systems.

Recently, researchers have focused on analyzing macro and micro energy systems using the second law of thermodynamics [20–22]. These analyses include, but not limited to, entropy generation rate in microchannels [21,23], concentric micro-fin tube heat exchangers [7], microcombustors [24,25] and microreactors [26,27]. These entropy generation rate analyses have even been extended to micro-thermoelectric layers [28] and micro thermoelectric cooling systems [29], where the Peltier effect has been incorporated into the formulation of entropy generation rate [28,30]. In addition to the analysis of entropy generation rate, a new method called Entropy Generation Minimization was introduced in Ref. [31]. In this method, different operating conditions are examined and the operating condition that minimizes entropy generation rate is identified. This method has been applied to different micro energy systems such as microchannels [32] and microreactors [33]. Although the heat transfer fundamental equations for steady-state micro systems are similar to that of macro systems, i.e., systems with a length scale larger than 1 meter [34,35], they differ significantly when transients are considered [36,37]. Inclusion of transients in second law of thermodynamics analysis results in a different fundamental equation for entropy generation rate [36]. Beside effects of transients, other phenomena such as the temperature jump at interface [38] or heat generation rate due to the nonlinear drag coefficient [39] may reveal an important impact on the entropy generation rate in micro systems. Hence, they should be included in the mathematical description and simulation. While there is one review on the entropy generation rate in microchannels [40], there is a

substantial need for a more comprehensive review in connection with the entropy generation rate in micro thermal systems. These micro thermal and thermochemical systems are being increasingly used in physicochemical systems involving electrical [41], magnetic [42,43], multiphase [44,45] and chemical [3,46] effects. The interactions of these effects with the thermal and fluidic processes in microsystems and the subsequent thermodynamic modifications set a complex area of research. Such complexities go beyond the first law of thermodynamics and should be covered by the second law investigations. Therefore, this article provides a thorough literature survey on the second law analysis of micro thermal and thermochemical systems and, identifies the key relevant problems for further research.

This review is divided into six sections. Following the introduction, Section 2 provides fundamental equations for entropy generation rate. The concept of generation of entropy in single- or multiphase flow in microchannels is then discussed in Section 3. Section 4 reviews investigations related to the entropy generation rate inside microchannels considering magnetic and electric effects, while Section 5 presents entropy generation rate in nanofluid flow through microchannels. Section 6 discusses the entropy generation rate in microreactors and microcombustors. Finally, Section 7 presents the conclusions and suggested areas for future work.

2. Fundamental formulations

Entropy generation rate is determination of the irreversibilities encountered in a specific process. To obtain the total generation of entropy in a thermofluidic system at the system level, the following general equation for a control volume medium is given as:

$$dsdt = msin - msout + QT + Sgen,tot\ , \tag{1}$$

This equation, as it is seen from the left-hand side, provides the real-time entropy generation rate of a process. The first and second terms on the RHS are total entropy flow into and out of the system, respectively and the third term provides the entropy production because of internal heat generation rate. With simplifying assumptions such as steady-state and no heat generation rate in the system, the total entropy generation rate is the difference between entropy flow out of and into the system. Assuming that the process under investigation is a microchannel condenser [47] which uses air and R134a as the refrigerant, Eq. (1) reduces to Eq. (2) as follows:

$$Sgen,tot = segmentmasa,out - sa,in + mrsr,out - sr,in. \tag{2}$$

The local entropy generation rate of the subsystem, is defined using partial differential equations from which the entropy production at any specific location of the system is determined. For example, considering a simple two-dimensional microchannel with a fluid is passing through the microchannel and absorbing heat from the walls as shown in Fig. 1, the partial differential equation for energy transfer of the fluid is written as follows [48]:

$$\rho c_p u \frac{\partial T}{\partial x} = k \frac{\partial^2 T}{\partial y^2} + \mu \left(\frac{du}{dy}\right)^2 . \quad (3)$$

Following Ref. [31] the local entropy generation rate is formulated as:

$$S''' = k\left[\left(\frac{\partial T}{\partial x}\right)^2 + \left(\frac{\partial T}{\partial y}\right)^2\right] + \frac{\mu}{T}\left(\frac{\partial u}{\partial y}\right)^2 . \quad (4)$$

The above formulation can be extended for a porous microchannel. Assuming the microchannel contains porous material, the local entropy generation rate within the porous region is obtained via [49]:

$$S''' = k_m\left[\left(\frac{\partial T}{\partial x}\right)^2 + \left(\frac{\partial T}{\partial y}\right)^2\right] + \frac{\mu_\kappa}{T}u^2 + \frac{\mu}{T}\left(\frac{\partial u}{\partial y}\right)^2 . \quad (5)$$

On the RHS of Eq. (5) the second and third terms show the impact of the porous medium, including the fluid effective thermal conductivity and viscosity. This equation is developed based on the local thermal equilibrium (LTE) approach, which assumes equal local temperature for both solid phase and fluid phase of the porous medium. Hence, one thermal characteristic is assumed for the porous medium. There are physical conditions in porous media where the LTE approach is not valid. For example, when the thermal conductivity of the fluid and solid phases differs significantly or considerable heat generation rate exists in any of these phases, the LTE assumption breaks down. Accordingly, a two temperature model, which is also referred to as the local thermal non-equilibrium (LTNE) model, is applied for heat transfer analyses of porous media [50,51]. Using the LTNE approach, the partial differential equations for a two-dimensional thermofluidic porous system to calculate local entropy generation rate is governed by the following relations [52]:

$$S_f''' = k_{ef}\left[\left(\frac{\partial T_f}{\partial x}\right)^2 + \left(\frac{\partial T_f}{\partial y}\right)^2\right] + h_{sf} a_{sf}(T_s - T_f) + \frac{\mu_\kappa}{T_f}u_f^2 + \frac{\mu}{T_f}\left(\frac{\partial u_f}{\partial y}\right)^2, \quad (6a)$$

$$S_s''' = k_{es}\left[\left(\frac{\partial T_s}{\partial x}\right)^2 + \left(\frac{\partial T_s}{\partial y}\right)^2\right] - h_{sf} a_{sf}(T_s - T_f). \quad (6b)$$

As shown in several recent investigations, integration of the local rate of entropy generation in the solution domain results in the total rate of entropy generation [53,54]. Even though the sub-system analysis is computationally demanding and rigorous compared to the system perspective, it provides detailed insight within the quality of the thermal process and the exact location of features with high or low entropy generation rate. Altogether, the sub-system perspective can be a more powerful tool than the system perspective for the Second Law optimization. Given this brief overview of the formulation of entropy generation rate and different perspectives, the following section presents a thorough discussion of the recent system and sub-system entropy generation rate investigations for micro thermofluidics.

3. Entropy generation rate in single-phase and multiphase flows in microchannels

Fundamentally, the fluid flow and heat transfer in microchannels can be classified to two categories, single-phase and multiphase flows [55]. Single-phase flows are, themselves, categorized in two groups. The first includes single component flows, such as CO_2 or water vapor passing through a microchannel. The second, involves multi-component flows, such as dry air and water vapor flows through a microchannel [55]. This

sub-category is also applied to multiphase flows as both single component and multi-component two-phase and multiphase flows are possible [55–57].

Recently, single-phase and multiphase fluid flow and heat transfer analyses of microchannels have received significant attention [58,59], and researchers have performed both numerical [45,60–62] and experimental [45,60,62] investigations in these regimes. The primary focus to date has been on the First Law analysis of these systems. Nonetheless, one of the most classical categories of studies on entropy generation rate in micro systems is entropy generation rate in single-phase and multiphase flows in microchannels. Recently, several investigations have been done in this area [7,26,27,32,63–66]. The analysis of entropy generation rate of single-phase flows in microchannels [7,26,27,32,63–65] is fairly straightforward compare to that of multiphase flows [47,65,66]. In both of these categories, the entropy generation rate is either evaluated by solving ordinary or partial differential equations, i.e., sub-system modeling [26,27,32] or by simple algebraic equations, i.e., system modeling [7,47,65]. Depending on the complexity of the problem and the simplifying assumptions, the differential equations for single-phase flow, analyses of entropy generation rate can be solved analytically [26,27] or numerically [32,64]. As noted in Section 2, when the analysis of entropy generation rate is considered, i.e., solving the differential equations, both local and total rate of entropy generation results are available and there is an opportunity to identify the specific thermophysical property of the microchannel that results in the greatest entropy production rate, i.e., exergy destruction. However, the local rate of entropy generation analysis of multiphase flows in microchannels is more challenging due to the complex mathematical modelling and phenomenological character of the flow [67–69]. Hence, the second simulation approach, i.e., system model, is mostly used for the analysis of entropy generation rate in microchannels with multiphase flow [47,65] or concentric heat exchangers [7]. In this approach, only the input and output characteristics of the fluid are considered. Depending on the assumptions, thermophysical properties and components of the system, Eq. (2) which correlates the specifications of a thermofluidic system to the total rate of entropy generation is discussed.

As an example, consider the first term of the RHS of Eq. (2). By writing the entropy generation rate equations for the air at the inlet and outlet using temperature and pressure, the total rate of entropy generation of the air within the system is determined. Assuming air as an ideal gas and constant specific heats the refrigerant entropy change is expressed as [47]:

$$\dot{S}_{gen,a}=\dot{m}_a s_{a,out}-s_{a,in}=\dot{m}_a c_{p,a}\ln\frac{T_{a,out}}{T_{a,in}}-R\ln\frac{P_{a,out}}{P_{a,in}} \tag{7}$$

For determination of the entropy generation rate of refrigerant some additional analysis is required. Here, the role of the pressure drop of the refrigerant on the entropy generation rate is discussed. Applying Gibbs relation $Tds=di-vdP$, the entropy variation for the refrigerant is expressed as:

$$ds=\frac{di}{T}-\frac{v}{T}dP\quad\Rightarrow\quad\frac{ds}{dT}=\frac{di}{dT}-\frac{1}{\rho T}\frac{dP}{dT}. \tag{8}$$

The total entropy generation rate because of pressure drop is represented by the second term in Eq. (8). The total impact of the air and refrigerant is expressed as:

$$S_{gen,\Delta P} = \dot{m}_{r,segment} \Delta P_r T_r \rho_r - \dot{m}_{a,segment} R \ln \frac{P_{a,out}}{P_{a,in}} \quad (9)$$

Similarly, the entropy generation rate because of heat transfer for the air and the refrigerant is formulated using Eq. (10)

$$S_{gen,ht} = segment \dot{m}_a c_{p,a} \ln \frac{T_{a,out}}{T_{a,in}} + \dot{m}_{r,out} - \dot{m}_{r,in} - \dot{m}_r \Delta P_r T_r \rho_r \quad (10)$$

The first term on the RHS of Eq. (10) is the entropy generation rate because of heat transfer for the air and the other terms represent entropy generation rate for the refrigerant. In Eq. (10), presents the total entropy generation rate from the refrigerant with the pressure drop source term removed to achieve the entropy generation rate because of heat transfer. In this expression represents the pressure drop for the refrigerant and is positive in Eq. (10). By solving the appropriate equations for a microchannel-condenser, the total rate of entropy generation through the microchannel is determined. Since this method does not provide any information about the local rate of entropy generation in the microchannel, there is only limited opportunity to identify physical causes for the entropy generation rate at a specific point in the system, and hence it provides less information by which the entropy generation rate is assessed and optimized. For example, Fig. 2 illustrates the different components of entropy generation rate including the pressure drop entropy generation number for air (N_a_pd), the pressure drop entropy generation number for refrigerant (N_r_pd), heat transfer entropy generation number (N_ht), and the total entropy generation number (N_tot) versus mass flow rate of air inside a microchannel condenser. It is apparent that while the total entropy generation number is optimized for a particular mass flow rate, information on the local entropy generation rate is missing [47]. That said, this section of the review is divided into two sub-sections to discuss each of these categories in depth, based on a system or sub-system approach. Here, Table 1 is provided to concisely summarize the above literature review.

3.1. Entropy generation rate in single-phase flows

As previously discussed, when single-phase flow is available in a microchannel, the typical approach is solving the Navier-Stokes and energy governing equations. Hence, it is possible to obtain both local and total entropy generation rates and perform entropy generation minimization. Since the configuration of interest here is a microchannel, the walls' thickness of the microchannel can be similar to the clear/porous part of the microchannel [63,70]. In that case, the thermal analyses should consider the wall geometry. In Section 2, the fundamental entropy generation rate equations for open microchannels, and porous microchannels, considering both LTE and LTNE approaches were discussed via Eqs. (4)-(6b). In this section, the formulation of the entropy generation rate will be expanded to a partially porous microchannel.

Assuming a partially filled porous microchannel as shown in Fig. 3, the momentum and energy governing equations can be simplified and solved analytically. The momentum governing equations in the open and porous parts are written as

$$-\partial p\partial x+\mu eff\partial 2uf1\partial y2-\mu f\kappa uf1=0 \qquad h1\le y<h2, \tag{11a}$$

$$-\partial p\partial x+\mu f\partial 2uf2\partial y2=0 \qquad h2\le y\le h3 \tag{11b}$$

respectively. Equation (11a) is referred to as the Darcy-Brinkman model for momentum transfer in porous media [71]. Assuming the LTNE model within the porous media, the energy governing equations in fluid and solid phases are expressed as:

$$k1ddydT1dy+q1=0 \qquad 0<y\le h1, \tag{12a}$$

$$\rho cpuf1\partial Tf1\partial x=kef\partial 2Tf1\partial y2+hsfasfTs-Tf1+sf \qquad h1\le y<h, \tag{12b}$$

$$0=kes\partial 2Ts\partial y2-hsfasfTs-Tf1+ss \qquad h1\le y<h2, \tag{12c}$$

$$\rho cpuf2\partial Tf2\partial x=kf\partial 2Tf2\partial y2+sf \qquad h2\le y\le h3, \tag{12d}$$

$$k2ddydT2dy+q2=0 \qquad h3<y\le h4 \tag{12e}$$

As seen from Eqs. (12a) and (12e), the energy governing equations for the microchannel solid walls have been incorporated in the formulations. It is worth noting that this approach is different to the so called 'pore-scale modelling' which is more precise but highly computationally demanding. This is important once the wall thickness of the microchannel is comparable to dimensions of the open/porous section [70], where heat transfer in the wall affects the thermal features and entropy generation rate of the microchannel. Recently, effects of microchannels' walls on the entropy generation rate have been evaluated in several investigations [26,72–74]. It was shown that normal heat transfer through walls has a substantial impact on the total heat transfer and entropy generation rate of the microchannels [26,72–76]. It should be mentioned that Eq. (12) can be easily transformed to be applicable for the LTE model in porous media [77]. This is accomplished by first approximating the interstitial heat transfer coefficient between the fluid and solid phases of the porous medium, i.e., , by a relatively high value. This approximation initially overestimates the thermal interaction between the two-phases and allows the values to be iterated to ultimately unify the temperature of the two-phases in the porous section.

The analyses of entropy generation rate in porous microchannels were performed with different physical conditions such as temperature jump/velocity slip boundary conditions at porous-wall interface, and generation/absorption of heat within microchannel. Some researchers [26,27] computationally investigated entropy generation rate of single-phase flow in porous microchannels using an LTNE model. In some cases, the exothermic and endothermic effects were incorporated into the simulation, where microchannels were

asymmetric [26,27]. In another numerical study, when an LTE approach was considered, the temperature jump and velocity slip interface boundary conditions were incorporated [63,78]. Some investigations considered a microchannel with relatively thick walls occupied with porous materials in which different wall-surrounding interface boundary conditions were considered. Figure 4 illustrates the two different cases investigated [78]. Because a temperature jump parameter was incorporated at the fluid-solid interface, the entropy generation rate for each solid-fluid interface in the microchannel was readily determined using calculation of the entropy generation rate of each phase separately, i.e., the ratio of heat flux to that of the temperature of the specific medium. Hence, the entropy generation rate at the interface was formulated as [78]:

$$Si = Qi\,lTi,s - lTi,f \tag{13}$$

It was shown that while rising the temperature jump boundary condition reduces the local rate of entropy generation [63], it may eventually rise up the total rate of entropy generation of the system [78]. Several computational fluid dynamics simulations address the entropy generation rate in single-phase flows through microchannels [32,64]. These simulations examined clear microchannels using different triangular cavities at the sidewalls. Two configurations are shown in Fig. 5. In these cases, the Reynolds number is a determining parameter for minimizing the entropy generation rate [32]. In an interesting study of the experimental and numerical entropy generation rate [7], a horizontal concentric micro-fin tube heat exchanger was analyzed. This study demonstrated that the numerically predicted data could accurately approximate the experimental results.

3.1.1. Entropy generation rate in single-phase multi-component flows

Entropy generation rate in single-phase multi-component flows such as airflow through microchannels was studied in different investigations [79–82]. In a theoretical investigation [79], studies were reported on entropy generation rate in hydrodynamically and thermally fully developed airflow through parallel plate microchannels with asymmetric heat fluxes on top and bottom walls. It was shown that entropy generation rate increases with decreasing Peclet number for Peclet numbers less than 10. This augmentation in entropy generation rate is because of significance of axial temperature gradient at low Peclet numbers [79]. However, as Peclet number increased to more than 10, effects of radial temperature gradient dominated axial temperature gradient and entropy generation rate remained constant. This study showed that sharp temperature gradients at microchannels' walls bring maximum entropy generation rate for different heat fluxes at walls. In a numerical investigation [80], entropy generation minimization was performed for laminar and steady airflow through bundles of microchannel. It was shown that total rate of entropy generation is higher for airflow with no-slip boundary condition than airflow with velocity slip boundary condition. This higher entropy generation rate is due to high velocity gradient close to wall. Further, it was concluded that for each operating condition there is a particular airflow rate that results in Entropy Generation Minimization in

microchannels. In another theoretical work [81], entropy generation rate of airflow between two parallel plates with symmetric heat fluxes was studied. This study showed that rate of entropy generation decreases across channel, and maximum entropy generation rate occurs at wall of micro- and macroscale channels. It was also shown that the total rate of entropy generation is higher and thermal interaction is lower in macroscale channels compared to microscale channels. For example, decreasing channel size from macroscale to microscale showed 50% reduction in the entropy generation rate and 50% enhancement in heat transfer. Investigations on Entropy Generation Minimization of moist air flow through bundles of microchannels were reported in Ref. [82]. Moisture transfer irreversibilities were included in entropy generation rate by heat transfer. The study showed that the entropy generation rate is minimized at specific values of air volume flow rate. For examples, the entropy generation rate is minimized in microchannels when air volume flow rate is $4\times10-3(m3s)$. Further, results showed that rising relative humidity of moist air increases convective heat transfer coefficient and decreases the entropy generation rate of airflow. For example, as relative humidity was intensified from 0 to 0.9, convective heat transfer coefficient was enhanced by 20 % and entropy generation rate decreased by 2.1 % [82].

The above studies [79–82] have provided useful information on the entropy generation rate of airflow through empty microchannels. However, effects of inserts in microchannels and enhanced heat and mass exchanges on the entropy generation rate have remained unstudied and form a gap in the literature. As inserts are used for simultaneous enhancement of heat transfer and mass transfer, it is predicted that the enhanced heat and mass transfer will result in considerable generation of entropy. Therefore, experimental and numerical study of entropy generation rate in microchannels with inserts will be a new research topic for thermal and fluid researchers.

3.2. Entropy generation rate in multiphase flows

A few studies on second law analysis of multiphase flow in microchannels are available in the literature, but these have recently attracted some additional attention [47,65,66]. As mentioned previously, these investigations have been primarily focused at the system level, and hence there are no partial differential equations to be considered [47,65,66]. As these analyses considered algebraic equations for determination of the entropy generation rate in the microchannels, the total entropy generation rate can be readily obtained [47,65]. While considering algebraic equations to obtain the total rate of entropy generation lacks the sense of completeness and detailed analysis, it provides a quick and reasonably accurate methodology by which the level of exergy destruction is determined. For example, it has been shown that under different thermophysical conditions, increasing the mass flow rate in a microchannel accommodating multiphase flow may increase, decrease, or not change the total entropy generation rate [47]. Figure 6 illustrates changes in the entropy generation rate with mass flow rate at different heat fluxes, in an evaporator as investigated in Ref. [65]. Based on this study, it is apparent that the entropy generation rate remains constant with augmenting mass flow rate and goes up with increasing heat flux. In a numerical investigation [66],

optimization of number of micro-fins in tube-in-tube heat exchangers with respect to thermophysical properties of the heat exchanger was discussed. The impact of number of micro-fins on heat transfer and pressure drop contributions to entropy generation rate are provided in Fig. 7. Evaluating the above-mentioned systems [47,65,66] based on a local rate of entropy generation perspective, requires examination of the partial differential equations, which are an inherent part of the heat and mass transport in multiphase and phase change systems [55]. That is one of the main reasons why micro thermal systems accommodating multiphase flows have not gained much attention for subsystem second law analyses, i.e., investigations on the local rate of entropy generation. As multiphase flows have found more and expanded applications in chemical and biocatalytic reactors [83] and nanoparticle-laden flows [84], now may be the time for concentrating on the system and sub-system second law analyses of multiphase flows and exergetic performances of systems with multiphase phenomena.

4. Entropy generation rate in microchannels in the presence of magnetic or electric fields

If a fluid is electrically conductive, the electric current can be transferred through the fluid using two specific mechanisms at two different regions of the system [85]. This idea has been used to develop a variety of "tools" in thermofluidic technologies, i.e., electromagnetic pumps [86–88]. This technique has found various applications in biological systems, such as those in miniaturized magnetic cell sorters [42].

The electromagnetic effects on the fluid flow and heat transfer in microchannels were investigated for a number of years [85,89]. As has been previously shown, both electric and magnetic resultant forces may influence the thermophysical properties of the system [88,89]. The main force occurring in microchannel fluid flow comes from the interplay of the electric current density and the magnetic field, which generates the Lorentz body force [92]. Several research works have investigated thermophysical characteristics of electromagnetic microchannels [93,94]. However, investigations on the entropy generation rate within microchannels in which electromagnetic forces play a role are quite limited. To date, two microchannel geometries with electromagnetic forces have been considered for analyses of entropy generation rate. These are shown in Fig. 8 [95,96]. In a numerical work [95], the studies reported on thermal characteristics of thermally developed nanofluid flow within a parallel plate microchannel, including effects of pressure-driven and streaming potential, i.e., resulting from the induced electric field. The effects of the electric field generated by streaming potential in the momentum and energy equations as well as the governing equations of entropy generation rate were considered. The local and total entropy generation rates of the microchannel at different nanoparticles concentration rate and Brinkman number were provided. It was discussed that the entropy generation rate increases and decreases with the Brinkman number and nanoparticles concentration, respectively, as shown in Fig.9. A research gap found in Ref. [95] is lack of information on variation of entropy generation rate with electro-kinetic parameters, which needs to be investigated.

In a relatively new investigation [96], comprehensive analyses provided on the entropy generation rate in a narrow fluidic microchannel induced by a uniform peristaltic wave under electro-kinetic force and magnetic field. While the well-known Poisson-Boltzmann equation for electric potential in the microchannel was used, both electrical and magnetic effects were incorporated in momentum, energy and entropy generation rate governing equations [96]. This study discussed the effects of Joule heating parameter and Hartmann number on the local entropy generation rate and local Bejan number. Figure 10 illustrates that the local entropy generation rate goes up with Joule heating parameter and Hartmann number along the microchannel. However, Fig. 10 (b) illustrates that the local entropy generation rate reduces with Hartmann number at the end of microchannel, e.g. y=0.95.

5. Entropy generation rate in nanofluid flow through microchannels

One of the most effective methods of increasing the Nusselt number is augmentation of fluid thermal conductivity of the fluid by incorporating nano-size particles to the fluid [97]. Because the thermal conductivity of the added nanoparticles, which usually are metal or their oxides [98–100], are greater than the thermal conductivity of the base fluid, the mean value of fluid thermal conductivity substantially increases. The suspension of fluid and nanoparticles is called nanofluid. So far, the application of nanoparticles in heat transfer augmentation in microchannels has been examined experimentally [101,102] and numerically [103–108] by several scholars. In an interesting work [109], nanofluids have even been considered for nano-drug delivery. However, the number of investigations regarding the second law performance of micro systems, while containing nanofluids is relatively small [21,29,110–112].

5.1. Single-phase mixture modeling approach

Following the investigation of the First Law performance of micro thermal systems involving nanofluids [105,108], some scholars started to re-examine these systems and effects of nanoparticles on the system from an entropy generation perspective [53,106,107]. The impact of Al_2O_3-water nanofluids on the performance of thermoelectric modules was analyzed in Ref. [29]. This study illustrated that at low Reynolds numbers, the total entropy generation rate of the thermoelectric module decreases when a small volume fraction of nanoparticles is added to the base fluid in hot side of heat exchangers. Alternatively, at high Reynolds numbers, the nanoparticles are added to the base fluid in cold side of heat exchangers to decrease the total entropy generation rate. Results showed that at low Reynolds numbers, i.e., Re=10, decreasing the nanoparticle diameter reveals no impact on the total entropy generation rate. However, at Reynolds number 50 and beyond, as the nanoparticle diameter reduces, the total entropy generation rate in cold side and hot side of heat exchangers decreases and increases, respectively. In a series of numerical works [111,112], the entropy generation rate was analyzed in viscous dissipative nanofluid flows through porous microchannels. A two-dimensional analytical solution with an LTNE assumption was used and temperature and contours of entropy generation rate were provided. It was shown that determination of Reynolds number has a

significant effect on variation of the total entropy generation rate with the nanoparticle volume fraction. For example, at Re=20, the total entropy generation rate decreased with increasing nanoparticle volume fraction, while at Re=100, a reverse trend for entropy generation rate was observed.

In a numerical study [21], the entropy generation rate in nanofluid flow with streamwise conduction through microchannels was investigated. This study used LTE model and showed the total entropy generation rate for the porous microchannel versus various parameters such as the volume fraction of nanoparticles and the Peclet number. Similar to Ref. [111], results showed that variation of the total entropy generation number with changes in the nanoparticle volume fraction depends on the flow velocities (i.e., Peclet numbers in dimensionless form in this study). In another numerical study [110], MHD mixed convection and entropy generation rate in a 3D microchannel using Al_2O_3–water nanofluid was investigated. This study considered a clear microchannel and incorporated effects of wall thickness and magnetic field in the momentum and entropy generation rate governing equations. After validating results [110] with the literature for entropy generation rate through circular microchannels [113], the total entropy generation rate for the microchannel versus different aspect ratios, Reynolds numbers and volume fractions was determined. Figure 11 provides one sample of the results and demonstrates that while the total entropy generation rate reduces with intensifying Reynolds number, increasing the aspect ratio, i.e., the microchannel width to height ratio, reduces the total entropy generation rate. Further, results illustrated that intensifying the volume fraction of the Al_2O_3 nanoparticles decreases the total entropy generation rate of the microchannel at various Reynolds numbers studied. It should be noted that for all of the above studies, a single-phase mixture model has been assumed.

5.2. Two-phase mixture modeling approach

A more accurate model to be considered in nanofluid flows is the two-phase mixture model [114,115]. Although this approach is computationally more demanding, it provides information about the distribution of nanoparticles within the system [116,117]. Assuming different distribution of nanoparticles within the system allows scholars to incorporate these information within the energy equation, and finally obtain more accurate temperature distributions [118,119]. It has been illustrated in Ref. [119] that considering single-phase model of natural convection of nanofluids with either Boussinesq approximation or temperature dependent thermal properties results in non-negligible differences for the heat transfer enhancement compared to when two-phase mixture model is applied.

There are several studies on the second law performance of the heat transfer systems containing nanoparticles, using the two-phase mixture model. In a computational study [120], the impact of TiO_2-water nanofluid on the entropy generation rate of turbulent flow inside annuli was examined. After validating the Nusselt values of the numerical simulation with experimental results, authors provided a comprehensive analysis of the data related to the total entropy generation rate. It was shown that within a particular range of

the radius ratio, it is possible to obtain a specific Reynolds number to minimize the total entropy generation rate. The schematic of the annuli under consideration in Ref. [120], and a sample optimization analysis is shown in Fig. 12. In another computational study [118] two approaches, i.e., single-phase and two-phase mixture, were applied on the thermal performances of circular tube heat exchangers using a nanofluid. The total entropy generation rate was compared with different parameters, including the nanofluid volume fraction, the Reynolds number and the nanoparticle diameter. An important result was that the Eulerian two-phase model over predicts the entropy production because of the frictional dissipation, in comparison to other two-phase and single-phase models. This over prediction intensifies with incremental increases in the volume fraction and/or the diameter of the nanoparticles. More recently, some researchers [121] reported utilization of the two-phase mixture model for investigating effects of magnetic fields on the first and second law performance of a nanofluid filled cavity. The impact of Rayleigh number on the entropy generation rate due to heat transfer, along with the effect of the fluid friction and magnetic field, and total rate of entropy generation were discussed. As illustrated in Fig. 13 , while the total rate of entropy generation goes up with Rayleigh number, presence of the magnetic field decreases the total rate of entropy generation. This study showed useful impacts of the presence of magnetic fields for improving second law performance and causing less exergy destruction.

The preceding literature review illustrates that the investigations of impacts of nanofluids on the second law performance of micro thermofluidic systems are very limited. As in many micro thermal systems, such as those related to biology [38,120] the accuracy of the data is vital. Therefore, it is necessary to undertake a re-investigation of micro thermal systems with nanofluids, from first and second law perspectives using the two-phase mixture model.

6. Entropy generation rate in chemically reactive flows

Over the last two decades, micro-structured reactors (or microreactors) have found significant applications in energy conversion. Microreactors usually consist of microchannels that accommodate chemical reactions [10,123,124]. Thermochemical microreactors predominately include gas phase reactions, although in some cases the fluid can be two-phase flow [3,124,125]. Microreactors for energy purposes are extensively classified to two main groups of microcombustors and micro thermochemical reactors for fuel processing. The former is often used to energize micro photovoltaic systems [10,126–128] or micro-propulsion devices [123,129], while the latter is employed for the reforming of liquid and gaseous fuels, methanation and Fisher-Tropsch as well as partial oxidation processes [3,124,130]. Hydrogen is a common product of fuel processing in microreactors and is used in fuel-cells for decentralized power generation [10,124]. A common feature of all the stated applications is the requirement for high rate of thermal interaction with the microreactor. This is due to the intense exothermicity or endothermicity of the accommodated chemical processes such as the combustion and reforming of natural gas. Thus, thermal irreversibilities are often significant in thermochemical microreactors. Further, chemical and mass exchange irreversibilities are important origins

of entropy generation rate in reactive media. It follows that microreactors are likely to generate high levels of entropy and therefore will include major exergetic losses. Similar to that for other energy devices, the second law efficiency of microreactors is an essential indicator of their performance and can be used as a design guide. The following section provides an overview of the entropy generation rate formulations and literature on the evaluation of entropy generation rate and exergy loss in thermochemical microreactors. The principal findings and the outstanding challenges are identified, and recommendations are made for future research.

6.1. Formulation of entropy generation rate in reactive flows

The fundamental equations of entropy generation rate in multi-component, chemically reactive flows were developed by several authors [77,131,132]. Here, the derivations from Ref. [33] is presented as it has been exclusively developed for reactive flows in microreactors. The Gibbs relation for a mixture consist of n species can be expressed by the following equation

$$di=Tds-Pdvsp+i=1n\mu idYi, \tag{14}$$

where μi is the chemical potential for species *i*. Combining Eq. (14) with the balance of energy results in the development of an equation for the transport of entropy as,

$$TDsDt=DiDt-P\rho 2D\rho Dt-i=1n\mu iDYiDt. \tag{15}$$

In the derivation of Eq. (15) the body forces and transport of heat by concentration gradient (Dufour effect) were considered negligible. Further, it is important to note that in microreactors with clear microchannels (as opposed to those filled with a porous media) evaluation of the irreversibilities arising from thermal radiation requires a separate radiation analysis, which will be presented separately. The current derivation, therefore, ignores the radiation effects and Eq. (15) is expressed as,

$$\rho DsDt=1T\nabla.kmix\nabla T-1T\nabla.i=1n\hbar iJi+\phi T+1Ti=1n\mu i\nabla.Ji-1Ti=1n\mu iri\ . \tag{16}$$

Equation (16) includes the reversible mechanisms of entropy transfer and generation due to irreversibilities. This equation is modified to take the standard form of a transport equation,

$$\rho DsDt=\nabla.qT+1Ti=1n\mu iJi+1T2kmix\nabla T2-1T2i=1n\hbar i.Ji.\nabla T+\phi T-1Ti=1n\mu iri+1Ti=1nJi.1T\mu i\nabla T-\nabla\mu i, \tag{17}$$

where $q=kmix\nabla T-i=1n\hbar iJi.$ The terms in the RHS of Eq. (17) are expressed in the following forms:

$$sR=\nabla.qT+1Ti=1n\mu iJi \tag{18a}$$

$$sgen'''total=1T2kmix\nabla T2-1T2i=1n\hbar iJi\nabla T+\phi T-1Ti=1n\mu iri+1Ti=1nJi.[1T\mu i\nabla T-\nabla\mu i] \tag{18b}$$

Equation (18a) shows the transport of reversible entropy, while Eq. (18b) presents the total rate of entropy generation. Recalling that $\mu i=\hbar i-Tsi$ and $\nabla\mu i=\nabla\hbar i-T\nabla si-si\nabla T$, and some algebraic manipulations lead to the

following breakdown of the total rate of entropy generation to reaction, conduction, mass diffusion and viscosity [33].

$$sgen'''r=-1Ti=1n\mu iri \quad (19a)$$

$$sgen'''cond=1T2kmix\nabla T2 \quad (19b)$$

$$sgen'''diff=i=1n(\rho RiDim)\nabla Yi.\nabla XiXi+i=1nRiDTi[\nabla TT\nabla XiXi] \quad (19c)$$

$$sgen'''vis=\phi T \quad (19d)$$

Radiative heat transfer entropy generation rate is obtained separately, and includes the entropy generation rate due to absorption, emission and the scattering of thermal energy [133]. Assuming isentropic scattering and grey media, the following equations approximate the radiative heat transfer entropy generation rate in the gas and solid media [33].

$$sgen'''rad,s=1TR,s\alpha s4\pi Ib,s-Gs-1Ts\alpha s4\pi Ib,s-Gs \quad (20a)$$

$$sgen'''rad,g=1TR,g\alpha g4\pi Ib,g-Gg-1Tg\alpha g4\pi Ib,g-Gg \quad (20b)$$

The total rate of volumetric entropy generation within the microreactor includes contributions from reaction, heat conduction, mass diffusion (due to the mass and thermal gradients), viscous dissipation and radiation in the solid and gaseous zones.

$$sgen'''total=sgen'''r+sgen'''cond+sgen'''diff+sgen'''vis+sgen'''rad,s+sgen'''rad,g \quad (21)$$

Table 3 summarizes mathematical equations shown for entropy generation studies.

6.2. Entropy generation rate in microcombustors

Microcombustors are a peculiar type of combustion systems as they include flames in passages that are often well below the quenching distances. For this reason, thermal management is an essential part of microcombustor design and operation [10,123]. Given that in most miniaturized systems the surface-to-volume ratio is quite high, the heat losses and thus the heat transfer irreversibilities of these microcombustors are expected to be significant. Further, heat losses can affect the chemical reactions and thus alter the chemical irreversibilities, while the enhanced transport of mass in microchannels is expected to decrease the mass transfer irreversibility. It follows that the entropic behavior of microcombustors can be different to that of conventional combustion systems. The latter has been extensively investigated (see for example Ref. [134] for a literature review and Refs. [135,136] for the most recent developments), while studies on the former are less frequent. This section puts forward a review of literature on entropy generation rate in microcombustors.

An early second law analysis in microcombustors was reported in Ref. [137]. This work reported an analytical investigation and evaluated entropy generation rate in the flame zone under steady-state. The

analysis considered a cylindrical microcombustor and examined the impacts of the type and concentration of the fuel, the input temperature, and the microcombustor diameter. The mathematical equations were developed according to the reversible transport and forced convection terms in the entropy governing equation. It was shown that the least entropy generation rate occurs at the similar tube radius, normalized by the thickness of the flame for the all investigated parameters. Therefore, the difference between the entropy generated by lean to rich flames decreases with increasing the tube radius. This implied that the choice of fuel and oxidizer equivalence ratio are essential parameters in the analysis of entropy generation rate of microcombustors. Results showed that that operation close to the stoichiometric ratio is the minimum efficient operational regime from the second law of thermodynamics viewpoint. The findings also demonstrated that, hydrogen-air stoichiometric flames generate more entropy due to the higher energy content of hydrogen in comparison with methane and propane. Importantly, this study [137] did not discuss the influence of heat losses on the second law performance of system.

In an extensive computational study [33], entropy generation rate in a cylindrical, premixed hydrogen burning microcombustor was analyzed. A stoichiometric reaction with one step chemistry and discrete ordinates (DO) method for modelling of thermal radiation was employed. The study was concerned about finding the optimal values of the wall thermal conductivity for which the exergetic losses of the microreactor were minimized. This study examined a wide range of wall thermal conductivities and found that the optimal exergetic behavior occurred in the domain of 0.1-1.75 W/m.K. It was also reported that chemical reactions were the strongest origin for entropy generation rate, where the thermal conduction and mass diffusion effects were secondary, and the influence of thermal radiation and viscous diffusion were found to be comparatively negligible. Further, in another work [14], it was argued that the wall thickness did not affect the irreversibilities significantly and that the entropy generation mainly occurred due to the irreversibilities encountered in the gas phase medium.

The assumption of single step chemistry was removed in the subsequent work in Ref. [138], in which the multistep chemical kinetics of premixed hydrogen combustion were included in the numerical second law analysis of a cylindrical microcombustor. The results demonstrated that irreversibilities are spatially distributed in the volume of the microreactor and hence, precise modelling of transport phenomena downstream of the flame is of high significance. As a very interesting outcome, this study [138] demonstrated that the same group of reactions overcomes the heat generation rate and the entropy generation rate and the two most significant participating reactions include hydroperoxyl radical, HO_2. Further, it was shown that the affinity of a reaction and local temperature of the gaseous mixture govern the total entropy generation rate. Abrupt increases in the volumetric rate of entropy generation initiate from the cooler parts of the flame with temperatures varying from 400 and 700 K. These increases are strongly affected by the following reactions, $H+O_2+M=HO_2+M$ and $H+HO_2=2OH$. It was therefore concluded that the reduced order kinetics used in the studies on entropy generation rate of micro-combustion should be able to account for the low temperature heat release [138]. It was also shown that the entropy generation rates do not pursue the same trends as

flame temperature on the fuel rich side and instead increase monotonically for the equivalence ratios between 0.5 and 1.4. Total entropy generation rate declined close to the stoichiometric point when approached from either the lean or rich sides [138].

Entropy generation rate in premixed hydrogen microcombustors was also investigated in Ref. [24]. Using a reduced set of chemical kinetics, authors conducted a two-dimensional numerical study of exergetic losses in microcombustor equipped with a recuperator. A parametric study was conducted, revealing that the reduction of equivalence ratio monotonically decreases the exergy losses of the system. It was shown that alteration of the equivalence ratio from 0.5 to 1 could double the exergy destruction occurring inside the microreactor [24]. The study further showed that the incorporation of thermal recuperator can decrease the generation of entropy by around 40% and thus serve as an important mechanism for reducing the entropy generation rate of the system [24]. The same group of authors [25] investigated the effect of baffles on the second law performance of premixed H_2/air microcombustor with heat recuperation. It was shown that the increases in the height of the baffle leads to considerable intensification of the total rate of entropy generation in the system. Further, both lean and rich operation were found to result in better second law efficiencies in comparison with that of stoichiometric conditions [25].

The susceptibility of a flame in microcombustors to quenching and extinction due to heat losses has raised interest in heat recirculation mechanisms [10]. However, this may lead to an inflation of entropy generation rate as preheating of the reactants can sharpen the local temperature gradients considerably. To resolve this issue, a theoretical study [139] investigated a thick-wall, plug flow axisymmetric microcombustor under steady-state condition, on the basis of flame sheet assumption. The study used analytical approach for finding the thermal fields within solid and gas phases as well as the laminar flame speed and fuel mass fraction [139]. An exergy analysis was then conducted and resulted in the following conclusions. First, the irreversibilities were shown to be limited to a narrow region around the flame, similar to that reported in conventional flames. Second, it was shown that increases in heat losses have a moderately decreasing effect upon all type of exergy losses in the microcombustor. And third, heat recirculation was shown to result in the increase of the exergetic losses, while increases in the wall thickness, solid to fluid thermal conductivity ratio and Peclet number have similar effects [139]. Most recently, this analytical work was further expanded with the purpose of identifying the optimum condition for heat recirculation and the associated exergetic behavior of the microcombustor [140]. This study revealed that the exergy destruction at outer wall is between 5-7% of inflow exergy, and the processes of heat recirculation and combustion account for the destruction of around 40-45% of the inflow exergy. Results showed that the second law efficiency of microcombustor is nearly invariant close to the value of 58% [140].

Entropy generation rate in premixed microcombustors burning syngas ($CO+H_2$) was investigated numerically in Ref. [141]. Authors considered a circular cylinder microchannel and took into account the detailed chemistry of syngas combustion. This study showed that the addition of CO to the premixed

reactants suppresses the irreversibilities generated by the chemical reaction. It was further demonstrated that the reaction of $OH+H_2O=H+H_2O$ is the most irreversible reaction and therefore dominates the rate of chemical entropy generation. Nonetheless, the relative contribution of the reaction $CO+OH=CO_2+H$ rises up as the concentration of CO in the reactants increases. This investigation [141] reported calculation of the spatial distribution of entropy generation rate and clearly demonstrated the elongation of the flame and suppression of chemical entropy with addition of CO. The results showed that the total entropy generation rate increases with the inlet velocity.

In a novel study on micro-photovoltaic system [142], a parallel plate microreactor with a central plate was developed. The ultimate goal was to achieve a more uniform temperature distribution and a number of configurations were evaluated experimentally and numerically. This study identified a design that results in the most uniform temperature field and minimum entropy generation rate. The impact of the inlet pressure on the exergetic efficiency of a cylindrical, premixed hydrogen microcombustor were studied computationally in Ref. [143]. The microcombustor was one part of a micro-photovoltaic device and included a step for improved flame capturing. In this investigation, the inlet pressure of reactants showed a significant impact on the entropy generation rate in the reactive part. The system was estimated to feature a maximum exergetic efficiency of approximately 40% at an input gauge pressure of 0.1 MPa. Decreasing the inlet pressure to 0.06 MPa (gauge) was observed to result in more than a 4% reduction in the exergetic efficiency of the microcombustor.

A numerical study [144] reported the second law analysis of a planar, premixed air and methane microcombustor with hydrogen addition. Utilizing a detailed chemical analysis, it was shown that the addition of H_2 to methane, caused the entropy generation rates resulting from thermal conduction and mass diffusion to decline. Nonetheless, the irreversibility induced by chemical reaction appeared to be less sensitive to H_2 addition. Sensitivity analyses revealed that at low concentrations of hydrogen the reaction $CH_3+O=CH_2O+H$ governs the chemical irreversibility. Yet, further increase of hydrogen magnifies the role of $H+O_2+M=H_2O+M$ and at 20% hydrogen content, this reaction becomes the most significant source of chemical irreversibility. In keeping with the earlier studies, results showed that the total entropy generation rate goes up as the inlet flow velocity increases. Further, the exergy destruction resulting from the wall heat losses is intensified by increasing the addition of hydrogen and the inlet velocity. It was shown that overall the exergetic efficiency of the microreactor remains almost constant with hydrogen addition [144]. Most recently, studies on energy and exergy performances of a microreactor used for photovoltaic applications were reported in Ref. [145]. This research found that the addition of a series of micro-fins makes the temperature distribution along the reactor more uniform and thus improves the exergetic behavior of the microcombustor. A separate study of microcombustors integrated with photovoltaic systems revealed that the geometric characteristics of the ribs implemented on the micro-reactor can considerably influence the entropy generation rate by changing the gas temperature [146]. In another recent numerical investigation, variations in the wall thickness of the microcombustor were found to be influential on the entropy generation

rate [147]. This study showed that a gradual decrease in the wall thickness and thus provision of a diverging microchannel, could lower the gas temperature and consequently reduce the entropy generation rate [147]. The results presented by Refs. [145,147] clearly reflect the significant effects of the solid body of microreactors on the second law performance of microcombustors. The high surface-to-volume ratio of microcombustors and the existence of very hot gases largely magnifies the share of solid body conduction in the generation of entropy. This finding presents an opportunity for improving the design of microcombustors that target entropy generation minimization.

Table 2 summarizes the investigations of the entropy generation rate in microcombustors. As shown, the existing investigations are exclusively focused on premixed combustion with a strong emphasis on hydrogen and hydrogen blends as fuel. Non-premixed micro-combustion has yet to be analyzed from the second law of thermodynamics viewpoint. In particular, the combustion of liquid fuels has been entirely excluded from the investigations of entropy generation rate. Given that combustion of liquids droplet involves complex entropy generation rate [134], extension of these studies to micro-combustion appears to be needed. Further, since catalytic combustion features strongly in micro-combustion [10], it is somewhat surprising that the irreversibility of catalytic reactions has received little attention in the investigation of either macro and microcombustors.

6.3. Entropy generation rate in thermochemical microreactors

Recently, there has been a fast-growing interest in utilization of microreactors to accommodate highly exothermic and endothermic processes for hydrogen and renewable fuel production [3,124]. High rates of transport, large surface area to volume ratios and compact size, as well as a reasonably straightforward way of scaling-up, are the main drivers of this interest. Fuel processing such as steam reforming of natural gas, methanation, hydrogenerations and carbon dioxide can include both heterogeneous (catalytic) and homogenous reactions, and often involves significant changes of the chemical enthalpy. These processes are fundamentally different from conventional combustion in the sense that they do not include sharp reaction zones such as those found in flames. This difference reveals an important effect on the entropy generation rates in more distributed reactions in microreactors when compared with microcombustors, which lead to the elimination of the sharp temperature gradients found in the flame region and is therefore expected to suppress thermal irreversibility.

The conversion of hydrocarbons to hydrogen (reforming reactions) and the production of hydrocarbons from carbon dioxides and hydrogen (e.g. methanation reaction) clearly involve chemical transformations and include significant heat exchange. As a result, the exergetic efficiencies of the process is an important performance indicator. Despite this apparent importance, there exists quite a few investigations on the entropy generation rate analysis of thermochemical microreactors. This may be explained by noting that the whole topic of thermochemical micro-reaction engineering is relatively new and developing [124].

The existing work in this area is limited to simple cases with one-step reactions, which may include internal heat generation/consumption rate. Some works [26,27] developed one-dimensional analytical models for heat transfer and entropy generation rate in thick wall, asymmetric microreactors. The microreactor was either totally or partially occupied by porous materials and could include internal heat generation rates in the fluid, solid phase of porous medium as well as the solid walls of the microreactor. Further, the configuration under investigation could feature different boundary conditions for temperature on the top and bottom surfaces. This study excluded mass transfer and found that the geometric and thermal asymmetry of the microreactor could significantly intensify the rate of entropy generation. Most recently, this investigation was expanded to cover thermal radiation and mass diffusion through the inclusion of a first order catalytic reaction at the internal walls of the microreactor [105,106]. These investigations [105,106] considered the thermal diffusion of mass using the Soret effect. It was found that the total rate of entropy generation is a function of the internal heat generation rate and by transition from an endothermic to exothermic system there are often minimal entropy generation rate points. Interestingly, it was demonstrated that the influence of thermal radiation upon the total irreversibility of the microreactor heavily depends on the thermal boundary condition [106].

The theoretical investigations of transport and entropy generation rate in microreactors were extended to two-dimensional analyses in a recent work reported in Refs. [75,148]. These investigations assumed non-local thermodynamic equilibrium [149–152] and developed a closed form, two-dimensional numerical approach for the momentum, heat and concentration distributions in a porous microreactor with thick walls. The reactor could include a homogenous [75] or heterogeneous [148] reaction, yet the rate of reaction was assumed to be temperature invariant. Further, thermal radiation and thermal diffusion of chemical species were taken into account. The investigation of entropy generation rate in these configurations revealed that, similar to that found in microcombustors, viscous irreversibilities have a small share of the total entropy generation rate. Further, it was found that the mass transfer is a strong source of irreversibility compared with heat transfer for most of the investigated cases. This is essentially due to the inclusion of the Soret effect, which is highly irreversible. It should be noted that studies in Refs. [75,148] assumed the chemical reactions to be reversible and therefore the calculated entropy generation rate was limited to that resulting from the transport phenomena. Figure 14 illustrates the spatial distribution of different source of entropy generation rate throughout microreactors with thick and uneven walls.

Most recently, some studies [153,154] advanced the previous analyses to catalytic microreactors hosting exothermic surface reactions and further considered the thermal radiation effects. It was shown that the surface heat release could considerably change the heat and mass transfer features of the microreactor, however, the entropic behavior of the catalytic microreactor was not significantly influenced by the addition of surface heat release. This is only the case for small to moderate rates of heat release and strong rates of heat addition, such those found in catalytic combustors, which are expected to change the entropic features of the microreactor.

In a series of recent investigations [154,155], the influence of non-Newtonian fluids upon transport and entropic behaviors of microreactors was analyzed. It was found that although the deviation from Newtonian fluid caused noticeable modifications in the thermal characteristics of the microreactors, the influence on the entropy generation rate was secondary. Once again, this was attributed to the dominant effects of the mass exchange, which is not strongly affected by the changes in the fluid properties.

Second law analysis of thermochemical micro-reactors is still in the very early stages. Chemical irreversibilities in these microreactors are poorly understood. In particular, exploring the transport and chemical irreversibilities arising from catalytic reactions (particularly exothermic and endothermic catalytic reactions) is an important area for further investigation. Finally, the entropy generation rate by a bundle of microreactors with an integrated cooling system or a combination of microcombustors and micro-reformers has remained entirely unstudied and deserves immediate attention. A summary of the existing research works on the second law analysis of microreactors are included in Table 2.

7. Conclusions and remarks

The level of interest in the Second Law Analysis of micro energy systems, i.e., energy systems with a length scale larger than 1 micrometer, especially micro thermofluidic and thermochemical systems has notably increased recently. With the current vision toward sustainability and efficiency of the thermal, thermofluidic and thermochemical systems, the second law analysis and efficiency of micro systems are of increasing importance and significance. As presented in this paper, there are many investigations on the entropy generation rate in microchannels, micro reactors and micro condensers. Some studies showed that as length scale reduces to micro size, 50 % enhancement in thermal interaction and 50 % decrease in entropy generation rate are obtained. The impact of various physical conditions, such as the thermal, fluidic, magnetic, and chemical effects have been considered in the analyses of micro systems, from both a system and sub-system perspective. However, there are still some important research gaps that need additional study and attention. These research gaps include the impacts of nanoparticles on the second law performance of thermofluidic systems from a two-phase model perspective, system analysis of a bundle of micro reactors from a Second Law perspective, irreversibilities of combustion of liquid fuels in microcombustors, and the consideration of radiation heat transfer on the second law performance of micro thermal and thermochemical systems. The pore-scale modeling for simulation of heat and mass transfer in porous media is one of the most promising avenues by which one could explore the entropy generation rate in micro porous thermofluidic and thermochemical systems. In addition to pore-scale approach, experimental and numerical study of entropy generation rate in single-phase multi-component flows such as airflow through microchannels with inserts and impact of enhanced heat and mass transport on entropy generation rate has remained unexplored. Thus, utilization of pore-scale modeling and studies on entropy generation rate of airflow through microchannels with inserts deserve further attention. Future studies on entropy generation rate in microchannels with inserts can be useful for the researchers interested in cooling and heating

systems. Analyses on entropy generation rate of such systems may assist with further optimization of HVAC systems.

References

[1] Jiang PX, Fan MH, Si GS, Ren ZP. Thermal-hydraulic performance of small scale micro-channel and porous-media heat-exchangers. Int J Heat Mass Transf 2001;44:1039–51. doi:10.1016/S0017-9310(00)00169-1.

[2] Yang WM, Chou SK, Chua KJ, Li J, Zhao X. Research on modular micro combustor-radiator with and without porous media. Chem Eng J 2011;168:799–802. doi:10.1016/j.cej.2010.12.083.

[3] Kolb G, Hessel V. Micro-structured reactors for gas phase reactions. Chem Eng J 2004;98:1–38. doi:10.1016/j.cej.2003.10.005.

[4] Li J, Jia J, Huang L, Wang S. Experimental and numerical study of an integrated fin and micro-channel gas cooler for a CO2 automotive air-conditioning. Appl Therm Eng 2017;116:636–47. doi:10.1016/j.applthermaleng.2016.12.140.

[5] Cao HS, Vanapalli S, Holland HJ, Vermeer CH, ter Brake HJM. A micromachined Joule–Thomson cryogenic cooler with parallel two-stage expansion. Int J Refrig 2016;69:222–31. doi:10.1016/j.ijrefrig.2016.06.023.

[6] Meng E, Hoang T. Micro- and nano-fabricated implantable drug-delivery systems. Futur Sci 2012;3:1457–67.

[7] Naphon P. Study on the exergy loss of the horizontal concentric micro-fin tube heat exchanger. Int Commun Heat Mass Transf 2011;38:229–35. doi:10.1016/j.icheatmasstransfer.2010.11.016.

[8] Wang X. Experimental Micro/Nanoscale Thermal Transport. Hoboken, New Jersey: Wiley; 2012.

[9] Bergman TL, Lavine AS, Incropera FP, DeWitt DP. Introduction to Heat Transfer. 6th ed. John Wiley and Sons, Inc.; 2011.

[10] Kaisare NS, Vlachos DG. A review on microcombustion: Fundamentals, devices and applications. Prog Energy Combust Sci 2012;38:321–59. doi:10.1016/j.pecs.2012.01.001.

[11] Chen XB, Sui Y, Cheng YP, Lee HP, Yu P, Winoto SH, et al. Mass transport in a microchannel enzyme reactor with a porous wall: Hydrodynamic modeling and applications. Biochem Eng J 2010;52:227–35. doi:10.1016/j.bej.2010.08.015.

[12] Wang K, Vafai K, Wang D. Analytical characterization of gaseous slip flow and heat transport through a parallel-plate microchannel with a centered porous substrate. Int J Numer Methods Heat Fluid Flow 2016;26:854–78. doi:10.1108/HFF-09-2015-0364.

[13] Lee J, Mudawar I. Fluid flow and heat transfer characteristics of low temperature two-phase micro-channel heat sinks - Part 1: Experimental methods and flow visualization results. Int J Heat Mass Transf 2008;51:4315–26. doi:10.1016/j.ijheatmasstransfer.2008.02.012.

[14] Li J, Chou SK, Li ZW, Yang WM. Experimental investigation of porous media combustion in a planar micro-combustor. Fuel 2010;89:708–15. doi:10.1016/j.fuel.2009.06.026.

[15] Ling L, Zhang Q, Yu Y, Wu Y, Liao S, Sha Z. Simulation of a micro channel separate heat pipe (MCSHP) under low heat flux and low mass flux. Appl Therm Eng 2017;119:25–33. doi:10.1016/j.applthermaleng.2017.03.049.

[16] Abdoli A, Jimenez G, Dulikravich GS. Thermo-fluid analysis of micro pin-fin array cooling configurations for high heat fluxes with a hot spot. Int J Therm Sci 2015;90:290–7. doi:10.1016/j.ijthermalsci.2014.12.021.

[17] Zhang K, Chou SK, Ang SS. Fabrication, modeling and testing of a thin film Au/Ti microheater. Int J Therm Sci 2007;46:580–8. doi:10.1016/j.ijthermalsci.2006.08.002.

[18] Li T, Wu L, Liu Y, Wang L, Wang Y, Wang Y. Micro-heater on membrane with large uniform-temperature area. Proc. IEEE Sensors Conf., 2006, p. 571–5.

[19] Gupta NK, Gianchandani YB. Porous ceramics for multistage Knudsen micropumps—modeling approach and experimental evaluation. J Micromechanics Microengineering 2011;21:095029. doi:10.1088/0960-1317/21/9/095029.

[20] Pang L, Wang M, Wang W, Liu M, Wang J. Optimal thermal design of a stacked mini-channel heat sink cooled by a low flow rate coolant. Entropy 2013;15:4716–31. doi:10.3390/e15114716.

[21] Ting TW, Hung YM, Guo N. Entropy generation of nanofluid flow with streamwise conduction in microchannels. Energy 2014;64:979–90. doi:10.1016/j.energy.2013.10.064.

[22] Torabi M, Zhang K, Karimi N, Peterson GP. Entropy generation in thermal systems with solid structures - A concise review. Int J Heat Mass Transf 2016;97:917–31. doi:10.1016/j.ijheatmasstransfer.2016.03.007.

[23] Elazhary AM, Soliman HM. Entropy generation during fully-developed forced convection in parallel-plate micro-channels at high zeta-potentials. Int J Heat Mass Transf 2014;70:152–61. doi:10.1016/j.ijheatmasstransfer.2013.10.060.

[24] Jiang D, Yang W, Chua KJ. Entropy generation analysis of H2/air premixed flame in micro-combustors with heat recuperation. Chem Eng Sci 2013;98:265–72. doi:10.1016/j.ces.2013.05.038.

[25] Jiang D, Yang W, Chua KJ, Ouyang J, Teng JH. Analysis of entropy generation distribution in micro-combustors with baffles. Int J Hydrogen Energy 2014;39:8118–25. doi:10.1016/j.ijhydene.2014.03.092.

[26] Elliott A, Torabi M, Karimi N. Thermodynamics analyses of porous microchannels with asymmetric thick walls and exothermicity: An entropic model of microreactors. J Therm Sci Eng Appl 2017;9:041013. doi:10.1115/1.4036802.

[27] Hunt G, Karimi N, Torabi M. Analytical investigation of heat transfer and classical entropy generation in microreactors - The influences of exothermicity and asymmetry. Appl Therm Eng 2017;119:403–24. doi:10.1016/j.applthermaleng.2017.03.057.

[28] Figueroa A, Vázquez F. Optimal performance and entropy generation transition from micro to nanoscaled thermoelectric layers. Int J Heat Mass Transf 2014;71:724–31. doi:10.1016/j.ijheatmasstransfer.2013.12.080.

[29] Mohammadian SK, Zhang Y. Analysis of nanofluid effects on thermoelectric cooling by micro-pin-fin heat exchangers. Appl Therm Eng 2014;70:282–90. doi:10.1016/j.applthermaleng.2014.05.010.

[30] Goupil C, Seifert W, Zabrocki K, Muller E, Snyder GJ. Thermodynamics of thermoelectric phenomena and applications. Entropy 2011;13:1481–517. doi:10.3390/e13081481.

[31] Bejan A. Entropy Generation Minimization: The Method of Thermodynamic Optimization of Finite-Size Systems and Finite-Time Processes. First edit. CRC Press; 1996.

[32] Li YF, Xia GD, Ma DD, Jia YT, Wang J. Characteristics of laminar flow and heat transfer in microchannel heat sink with triangular cavities and rectangular ribs. Int J Heat Mass Transf 2016;98:17–28. doi:10.1016/j.ijheatmasstransfer.2016.03.022.

[33] Jejurkar SY, Mishra DP. Effects of wall thermal conductivity on entropy generation and exergy losses in a H2-air premixed flame microcombustor. Int J Hydrogen Energy 2011;36:15851–9. doi:10.1016/j.ijhydene.2011.08.116.

[34] Zhao L, Liu LH. Entropy generation analysis of electro-osmotic flow in open-end and closed-end micro-channels. Int J Therm Sci 2010;49:418–27. doi:10.1016/j.ijthermalsci.2009.07.009.

[35] Ibáñez G, López A, Pantoja J, Moreira J. Entropy generation analysis of a nanofluid flow in MHD porous microchannel with hydrodynamic slip and thermal radiation. Int J Heat Mass Transf 2016;100:89–97. doi:10.1016/j.ijheatmasstransfer.2016.04.089.

[36] Dong Y, Guo ZY. Entropy analyses for hyperbolic heat conduction based on the thermomass model. Int

J Heat Mass Transf 2011;54:1924–9. doi:10.1016/j.ijheatmasstransfer.2011.01.011.

[37] Tzou DY. Macro- to Microscale Heat Transfer: The Lagging Behavior. Washington, DC: Taylor and Francis; 1997.

[38] Torabi M, Karimi N, Zhang K, Peterson GP. Generation of entropy and forced convection of heat in a conduit partially filled with porous media – Local thermal non-equilibrium and exothermicity effects. Appl Therm Eng 2016;106:518–36. doi:10.1016/j.applthermaleng.2016.06.036.

[39] Gaikwad HS, Mondal PK, Wongwises S. Non-linear drag induced entropy generation analysis in a microporous channel: The effect of conjugate heat transfer. Int J Heat Mass Transf 2017;108:2217–28. doi:10.1016/j.ijheatmasstransfer.2017.01.041.

[40] Awad MM. A reviewof entropy generation in microchannels. Adv Mech Eng 2015;7:1–32. doi:10.1177/1687814015590297.

[41] Salari A, Navi M, Dalton C. A novel alternating current multiple array electrothermal micropump for lab-on-a-chip applications. Biomicrofluidics 2015;9:014113. doi:10.1063/1.4907673.

[42] Pamme N, Wilhelm C. Continuous sorting of magnetic cells via on-chip free-flow magnetophoresis. Lab Chip 2006;6:974–80. doi:10.1039/b604542a.

[43] Horton M, Hong H, Li C, Shi B, Peterson GP, Jin S. Magnetic alignment of Ni-coated single wall carbon nanotubes in heat transfer nanofluids. J Appl Phys 2010;107:1–5. doi:10.1063/1.3428450.

[44] Yan YY, Zu YQ, Dong B. LBM, a useful tool for mesoscale modelling of single-phase and multiphase flow. Appl Therm Eng 2011;31:649–55. doi:10.1016/j.applthermaleng.2010.10.010.

[45] Zhou Y, Chang H, Qi T. Gas-liquid two-phase flow in serpentine microchannel with different wall wettability. Chinese J Chem Eng 2016;25:874–81. doi:10.1016/j.cjche.2016.10.006.

[46] Ziegenbalg D, Löb P, Al-Rawashdeh M, Kralisch D, Hessel V, Schönfeld F. Use of "smart interfaces" to improve the liquid-sided mass transport in a falling film microreactor. Chem Eng Sci 2010;65:3557–66. doi:10.1016/j.ces.2010.02.039.

[47] Turkakar G, Okutucu-Ozyurt T, Kandlikar SG. Entropy generation analysis of a microchannel-condenser for use in a vapor compression refrigeration cycle Göker. Int J Refrig 2016;70:71–83. doi:10.1016/j.ijrefrig.2016.06.028.

[48] Hooman K. Entropy generation for microscale forced convection: Effects of different thermal boundary conditions, velocity slip, temperature jump, viscous dissipation, and duct geometry. Int Commun Heat Mass Transf 2007;34:945–57. doi:10.1016/j.icheatmasstransfer.2007.05.019.

[49] Tasnim SH, Shohel M, Mamun MAH. Entropy generation in a porous channel with hydromagnetic effect. Exergy, An Int J 2002;2:300–8. doi:10.1016/s1164-0235(02)00065-1.

[50] de Monte F, Haji-Sheikh A. Bio-heat diffusion under local thermal non-equilibrium conditions using dual-phase lag-based Green's functions. Int J Heat Mass Transf 2017;113:1291–305. doi:10.1016/j.ijheatmasstransfer.2017.06.006.

[51] Lindner F, Mundt C, Pfitzner M. Fluid Flow and Heat Transfer with Phase Change and Local Thermal Non-equilibrium in Vertical Porous Channels. Transp Porous Media 2015;106:201–20. doi:10.1007/s11242-014-0396-2.

[52] Torabi M, Karimi N, Zhang K. Heat transfer and second law analyses of forced convection in a channel partially filled by porous media and featuring internal heat sources. Energy 2015;93:106–27. doi:10.1016/j.energy.2015.09.010.

[53] Guthrie DGP, Torabi M, Karimi N. Energetic and entropic analyses of double-diffusive, forced convection heat and mass transfer in microreactors assisted with nanofluid. J Therm Anal Calorim 2019;137:637–58. doi:10.1007/s10973-018-7959-3.

[54] Torabi M, Torabi M, Eftekhari Yazdi M, Peterson GP. Fluid flow, heat transfer and entropy generation analyses of turbulent forced convection through isotropic porous media using RANS models. Int J Heat Mass Transf 2019;132:443–61. doi:10.1016/j.ijheatmasstransfer.2018.12.020.

[55] Ghiaasiaan SM. Two-Phase Flow, Boiling, and Condensation: In Conventional and Miniature Systems. New York: Cambridge University Press; 2008. doi:10.1017/CBO9780511619410.

[56] Vialle S, Druhan JL, Maher K. Multi-phase flow simulation of CO2 leakage through a fractured caprock in response to mitigation strategies. Int J Greenh Gas Control 2016;44:11–25. doi:10.1016/j.ijggc.2015.10.007.

[57] Lei H, Li J, Li X, Jiang Z. EOS7Cm: An improved TOUGH2 module for simulating non-isothermal multiphase and multicomponent flow in CO2–H2S–CH4–brine systems with high pressure, temperature and salinity. Comput Geosci 2016;94:150–61. doi:10.1016/j.cageo.2016.06.011.

[58] Zhou J, Luo X, Feng Z, Xiao J, Zhang J, Guo F, et al. Saturated flow boiling heat transfer investigation for nanofluid in minichannel. Exp Therm Fluid Sci 2017;85:189–200. doi:10.1016/j.expthermflusci.2017.03.002.

[59] Kumar V, Paraschivoiu M, Nigam KDP. Single-phase fluid flow and mixing in microchannels. Chem Eng Sci 2011;66:1329–73. doi:10.1016/j.ces.2010.08.016.

[60] Dixit T, Ghosh I. Review of micro- and mini-channel heat sinks and heat exchangers for single phase fluids. Renew Sustain Energy Rev 2015;41:1298–311. doi:10.1016/j.rser.2014.09.024.

[61] Pan KL, Chen ZJ. Simulation of bubble dynamics in a microchannel using a front-tracking method. Comput Math with Appl 2014;67:290–306. doi:10.1016/j.camwa.2013.05.001.

[62] Yue J, Luo L, Gonthier Y, Chen G, Yuan Q. An experimental study of air-water Taylor flow and mass transfer inside square microchannels. Chem Eng Sci 2009;64:3697–708. doi:10.1016/j.ces.2009.05.026.

[63] Torabi M, Peterson GP. Effects of velocity slip and temperature jump on the heat transfer and entropy generation in micro porous channels under magnetic field. Int J Heat Mass Transf 2016;102:585–95. doi:10.1016/j.ijheatmasstransfer.2016.06.080.

[64] Zhai YL, Xia GD, Liu XF, Li YF. Exergy analysis and performance evaluation of flow and heat transfer in different micro heat sinks with complex structure. Int J Heat Mass Transf 2015;84:293–303. doi:10.1016/j.ijheatmasstransfer.2015.01.039.

[65] Turkakar G, Okutucu-Ozyurt T. Entropy generation analysis and dimensional optimization of an evaporator for use in a microscale refrigeration cycle. Int J Refrig 2015;56:140–53. doi:10.1016/j.ijrefrig.2015.04.003.

[66] Abdous MA, Saffari H, Barzegar Avval H, Khoshzat M. The study of entropy generation during flow boiling in a micro-fin tube. Int J Refrig 2016;68:76–93. doi:10.1016/j.ijrefrig.2016.04.008.

[67] Sun D, Garmory A, Page GJ. Simulation of inertial behavior of dilute particle flow in horizontal channel with Eulerian method of velocity-reassociated quadrature-based method of moments. Powder Technol 2016;304:157–63. doi:10.1016/j.powtec.2016.09.035.

[68] Liu Q, Wang W, Palm B. Numerical study of the interactions and merge of multiple bubbles during convective boiling in micro channels. Int Commun Heat Mass Transf 2017;80:10–7. doi:10.1016/j.icheatmasstransfer.2017.01.001.

[69] Moore BK, Pahinkar DG, Garimella S. Experimental and Analytical Investigation of Displacement Flows in Microchannels. Int J Heat Mass Transf 2017;112:745–57. doi:10.1016/j.ijheatmasstransfer.2017.04.044.

[70] Chen Y, Shen C, Shi M, Peterson GP. Visualization study of flow condensation in hydrophobic microchannels. AIChE J 2014;60:1182–1192. doi:10.1002/aic.

[71] Nield DA, Bejan A. Convection in Porous Media. 4th editon. New York: Speringer; 2013.

[72] Elliott A, Torabi M, Karimi N, Cunningham S. On the effects of internal heat sources upon forced convection in porous channels with asymmetric thick walls. Int Commun Heat Mass Transf 2016;73:100–10. doi:10.1016/j.icheatmasstransfer.2016.02.016.

[73] Torabi M, Torabi M, Bud Peterson GP. Entropy generation of double diffusive forced convection in

porous channels with thick walls and soret effect. Entropy 2017;19:171. doi:10.3390/e19040171.

[74] Torabi M, Zhang K. Temperature distribution, local and total entropy generation analyses in MHD porous channels with thick walls. Energy 2015;87:540–54. doi:10.1016/j.energy.2015.05.009.

[75] Hunt G, Torabi M, Govone L, Karimi N, Mehdizadeh A. Two-dimensional heat and mass transfer and thermodynamic analyses of porous microreactors with Soret and thermal radiation effects—An analytical approach. Chem Eng Process - Process Intensif 2018;126:190–205. doi:10.1016/j.cep.2018.02.025.

[76] Dickson C, Torabi M, Karimi N. First and second law analyses of nanofluid forced convection in a partially-filled porous channel – The effects of local thermal non-equilibrium and internal heat sources. Appl Therm Eng 2016;103:459–80. doi:10.1016/j.applthermaleng.2016.04.095.

[77] Torabi M, Karimi N, Peterson GP, Yee S. Challenges and progress on the modeling of entropy generation in porous media: A review. Int J Heat Mass Transf 2017;114:31–46. doi:http://dx.doi.org/10.1016.

[78] Torabi M, Zhang Z, Peterson GP. Interface entropy generation in micro porous channels with velocity slip and temperature jump. Appl Therm Eng 2017;111:684–93. doi:10.1016/j.applthermaleng.2016.09.148.

[79] Sadeghi A, Saidi MH. Second law analysis of slip flow forced convection through a parallel plate microchannel. Nanoscale Microscale Thermophys Eng 2010;14:209–28. doi:10.1080/15567265.2010.502924.

[80] Khan WA, Yovanovich MM, Culham JR. Optimization of microchannel heat sinks using entropy generation minimization method. Annu IEEE Semicond Therm Meas Manag Symp 2006;2006:78–86. doi:10.1109/stherm.2006.1625210.

[81] Avci M, Aydin O. Second-law analysis of heat and fluid flow in microscale geometries. Int J Exergy 2007;4:286–301. doi:10.1504/IJEX.2007.013395.

[82] Cruz JM, Amaya IM, Correa CR. Influence of moist air in copper heat sinks: Analysis through the entropy generation minimization criterion. Ing e Investig 2015;35:44–52. doi:10.15446/ing.investig.v35n3.49623.

[83] Haase S, Murzin DY, Salmi T. Review on hydrodynamics and mass transfer in minichannel wall reactors with gas-liquid Taylor flow. Chem Eng Res Des 2016;113:304–29. doi:10.1016/j.cherd.2016.06.017.

[84] Yu M, Lin J. Nanoparticle-laden flows via moment method: A review. Int J Multiph Flow 2010;36:144–51. doi:10.1016/j.ijmultiphaseflow.2009.08.006.

[85] Qian S, Bau HH. Magneto-hydrodynamics based microfluidics. Mech Res Commun 2009;36:10–21. doi:10.1016/j.mechrescom.2008.06.013.

[86] Kilani M, Khasawneh H, Badran A, Awidi A. Further development on a gentle electromagnetic pump for fluids with stress-sensitive microparticles. Sensors Actuators, A Phys 2016;247:440–7. doi:10.1016/j.sna.2016.06.031.

[87] Lemoff AV, Lee AP. AC magnetohydrodynamic micropump. Sensors Actuators, B Chem 2000;63:178–85. doi:10.1016/S0925-4005(00)00355-5.

[88] Jahromi AE, Miller FK. Development of a proof of concept low temperature 4He Superfluid Magnetic Pump. Cryogenics (Guildf) 2017;82:68–82. doi:10.1016/j.cryogenics.2016.08.008.

[89] Mistrangelo C, Bühler L. Magneto-convective flows in electrically and thermally coupled channels. Fusion Eng Des 2013;88:2323–7. doi:10.1016/j.fusengdes.2013.03.063.

[90] Jian Y. Transient MHD heat transfer and entropy generation in a microparallel channel combined with pressure and electroosmotic effects. Int J Heat Mass Transf 2015;89:193–205. doi:10.1016/j.ijheatmasstransfer.2015.05.045.

[91] Ranjit NK, Shit GC. Joule heating effects on electromagnetohydrodynamic flow through a peristaltically

induced micro-channel with different zeta potential and wall slip. Phys A Stat Mech Its Appl 2017;482:458–76. doi:10.1016/j.physa.2017.04.072.

[92] McWhirter J, Crawford M, Klein D. Magnetohydrodynamic flows in porous media II: Experimental results. Fusion Technol 1998;34:187–97.

[93] Hasan MI, Ali AJF, Tufah RS. Numerical study of the effect of channel geometry on the performance of Magnetohydrodynamic micro pump. Eng Sci Technol an Int J 2017;20:982–9. doi:10.1016/j.jestch.2017.01.008.

[94] Tan MHY, Geubelle PH. 3D dimensionally reduced modeling and gradient-based optimization of microchannel cooling networks. Comput Methods Appl Mech Eng 2017;323:230–49. doi:10.1016/j.cma.2017.05.024.

[95] Zhao G, Jian Y, Li F. Streaming potential and heat transfer of nanofluids in parallel plate microchannels. Colloids Surfaces A Physicochem Eng Asp 2016;498:239–47. doi:10.1016/j.colsurfa.2016.03.053.

[96] Ranjit NK, Shit GC. Entropy generation on electro-osmotic flow pumping by a uniform peristaltic wave under magnetic environment. Energy 2017;128:649–60. doi:10.1016/j.energy.2017.04.035.

[97] Bozorg M, Fasano M, Cardellini A, Chiavazzo E, Asinari P. A review on the heat and mass transfer phenomena in nanofluid coolants with special focus on automotive applications. Renew Sustain Energy Rev 2015;60:1615–33. doi:10.1016/j.rser.2016.03.027.

[98] Buongiorno J. Convective transport in nanofluids. J Heat Transfer 2006;128:240–50. doi:10.1115/1.2150834.

[99] Mahian O, Kianifar A, Heris SZ, Wongwises S. Natural convection of silica nanofluids in square and triangular enclosures: Theoretical and experimental study. Int J Heat Mass Transf 2016;99:792–804. doi:10.1016/j.ijheatmasstransfer.2016.03.045.

[100] Khoshvaght-Aliabadi M, Pazdar S, Sartipzadeh O. Experimental investigation of water based nanofluid containing copper nanoparticles across helical microtubes. Int Commun Heat Mass Transf 2016;70:84–92. doi:10.1016/j.icheatmasstransfer.2015.12.006.

[101] Lee J, Mudawar I. Assessment of the effectiveness of nanofluids for single-phase and two-phase heat transfer in micro-channels. Int J Heat Mass Transf 2007;50:452–63. doi:10.1016/j.ijheatmasstransfer.2006.08.001.

[102] Zhai YL, Xia GD, Liu XF, Li YF. Heat transfer enhancement of Al2O3-H2O nanofluids flowing through a micro heat sink with complex structure. Int Commun Heat Mass Transf 2015;66:158–66. doi:10.1016/j.icheatmasstransfer.2015.05.025.

[103] Malvandi A, Ganji DD. Brownian motion and thermophoresis effects on slip flow of alumina/water nanofluid inside a circular microchannel in the presence of a magnetic field. Int J Therm Sci 2014;84:196–206. doi:10.1016/j.ijthermalsci.2014.05.013.

[104] Ting TW, Hung YM, Guo N. Effects of streamwise conduction on thermal performance of nanofluid flow in microchannel heat sinks. Energy Convers Manag 2014;78:14–23. doi:10.1016/j.enconman.2013.10.061.

[105] Govone L, Torabi M, Wang L, Karimi N. Effects of nanofluid and radiative heat transfer on the double-diffusive forced convection in microreactors. J Therm Anal Calorim 2019;135:45–59. doi:10.1007/s10973-018-7027-z.

[106] Govone L, Torabi M, Hunt G, Karimi N. Non-equilibrium thermodynamic analysis of double diffusive, nanofluid forced convection in catalytic microreactors with radiation effects. Entropy 2017;19:690. doi:10.3390/e19120690.

[107] Torabi M, Dickson C, Karimi N. Theoretical investigation of entropy generation and heat transfer by forced convection of copper–water nanofluid in a porous channel — Local thermal non-equilibrium and partial filling effects. Powder Technol 2016;301:234–54. doi:10.1016/j.powtec.2016.06.017.

[108] Guthrie DGP, Torabi M, Karimi N. Combined heat and mass transfer analyses in catalytic microreactors

partially filled with porous material - The influences of nanofluid and different porous-fluid interface models. Int J Therm Sci 2019;140:96–113. doi:10.1016/j.ijthermalsci.2019.02.037.

[109] Kleinstreuer C, Li J, Koo J. Microfluidics of nano-drug delivery. Int J Heat Mass Transf 2008;51:5590–7. doi:10.1016/j.ijheatmasstransfer.2008.04.043.

[110] Hajialigol N, Fattahi A, Ahmadi MH, Qomi ME, Kakoli E. MHD mixed convection and entropy generation in a 3-D microchannel using Al_2O_3-water nanofluid. J Taiwan Inst Chem Eng 2015;46:30–42. doi:10.1016/j.jtice.2014.09.002.

[111] Ting TW, Hung YM, Guo N. Entropy generation of viscous dissipative nanofluid convection in asymmetrically heated porous microchannels with solid-phase heat generation. Energy Convers Manag 2015;105:731–45. doi:10.1016/j.icheatmasstransfer.2015.09.003.

[112] Ting TW, Hung YM, Guo N. Entropy generation of viscous dissipative nanofluid flow in thermal non-equilibrium porous media embedded in microchannels. Int J Heat Mass Transf 2015;81:862–77. doi:10.1016/j.ijheatmasstransfer.2014.02.041.

[113] Sohel MR, Saidur R, Hassan NH, Elias MM, Khaleduzzaman SS, Mahbubul IM. Analysis of entropy generation using nanofluid flow through the circular microchannel and minichannel heat sink. Int Commun Heat Mass Transf 2013;46:85–91. doi:10.1016/j.icheatmasstransfer.2013.05.011.

[114] Goodarzi M, Safaei MR, Vafai K, Ahmadi G, Dahari M, Kazi SN, et al. Investigation of nanofluid mixed convection in a shallow cavity using a two-phase mixture model. Int J Therm Sci 2014;75:204–20. doi:10.1016/j.ijthermalsci.2013.08.003.

[115] Akbari OA, Safaei MR, Goodarzi M, Akbar NS, Zarringhalam M, Shabani GAS, et al. A modified two-phase mixture model of nanofluid flow and heat transfer in a 3-D curved microtube. Adv Powder Technol 2016;27:2175–85. doi:10.1016/j.apt.2016.08.002.

[116] Garoosi F, Rohani B, Rashidi MM. Two-phase mixture modeling of mixed convection of nanofluids in a square cavity with internal and external heating. Powder Technol 2015;275:304–21. doi:10.1016/j.powtec.2015.02.015.

[117] Amani M, Amani P, Kasaeian A, Mahian O, Yan WM. Two-phase mixture model for nanofluid turbulent flow and heat transfer: Effect of heterogeneous distribution of nanoparticles. Chem Eng Sci 2017;167:135–44. doi:10.1016/j.ces.2017.03.065.

[118] Rashidi MM, Nasiri M, Shadloo MS, Yang Z. Entropy Generation in a Circular Tube Heat Exchanger Using Nanofluids: Effects of Different Modeling Approaches. Heat Transf Eng 2017;38:853–66. doi:10.1080/01457632.2016.1211916.

[119] Corcione M, Cianfrini M, Quintino A. Two-phase mixture modeling of natural convection of nanofluids with temperature-dependent properties. Int J Therm Sci 2013;71:182–95. doi:10.1016/j.ijthermalsci.2013.04.005.

[120] Siavashi M, Jamali M. Heat transfer and entropy generation analysis of turbulent flow of TiO2-water nanofluid inside annuli with different radius ratios using two-phase mixture model. Appl Therm Eng 2016;100:1149–60. doi:10.1016/j.applthermaleng.2016.02.093.

[121] Mohammadpourfard M, Aminfar H, Ahangar Zonouzi S. Numerical investigation of the magnetic field effects on the entropy generation and heat transfer in a nanofluid filled cavity with natural convection. Heat Transf - Asian Res 2017;46:409–33. doi:10.1002/htj.21222.

[122] Akbar NS, Butt AW. Entropy generation analysis in convective ferromagnetic nano blood flow through a composite stenosed arteries with permeable wall. Commun Theor Phys 2017;67:554–60. doi:10.1088/0253-6102/67/5/554.

[123] Ju Y, Maruta K. Microscale combustion: Technology development and fundamental research. Prog Energy Combust Sci 2011;37:669–715. doi:10.1016/j.pecs.2011.03.001.

[124] Kolb G. Review: Microstructured reactors for distributed and renewable production of fuels and electrical energy. Chem Eng Process Process Intensif 2013;65:1–44. doi:10.1016/j.cep.2012.10.015.

[125] Pennemann H, Kolb G. Review: Microstructured reactors as efficient tool for the operation of selective

oxidation reactions. Catal Today 2016;278:3–21. doi:10.1016/j.cattod.2016.04.032.

[126] Akhtar S, Khan MN, Kurnia JC, Shamim T. Investigation of energy conversion and flame stability in a curved micro-combustor for thermo-photovoltaic (TPV) applications. Appl Energy 2017;192:134–45. doi:10.1016/j.apenergy.2017.01.097.

[127] Alipoor A, Saidi MH. Numerical study of hydrogen-air combustion characteristics in a novel micro-thermophotovoltaic power generator. Appl Energy 2017;199:382–99. doi:10.1016/j.apenergy.2017.05.027.

[128] Amani E, Alizadeh P, Moghadam RS. Micro-combustor performance enhancement by hydrogen addition in a combined baffle-bluff configuration. Int J Hydrogen Energy 2018;43:8127–38. doi:10.1016/j.ijhydene.2018.03.016.

[129] Jejurkar SY, Mishra DP. Thermal performance characteristics of a microcombustor for heating and propulsion. Appl Therm Eng 2011;31:521–7. doi:10.1016/j.applthermaleng.2010.10.009.

[130] Götz M, Lefebvre J, Mörs F, McDaniel Koch A, Graf F, Bajohr S, et al. Renewable Power-to-Gas: A technological and economic review. Renew Energy 2016;85:1371–90. doi:10.1016/j.renene.2015.07.066.

[131] Arpaci VS, Selamet A. Entropy production in flames. Combust Flame 1988;73:251–9. doi:10.1016/0010-2180(88)90022-3.

[132] Nishida K, Takagi T, Kinoshita S. Analysis of entropy generation and exergy loss during combustion. Proc Combust Inst 2002;29:869–74. doi:10.1016/S1540-7489(02)80111-0.

[133] Liu LH, Chu SX. On the entropy generation formula of radiation heat transfer processes. J Heat Transfer 2006;128:504–6. doi:10.1115/1.2190695.

[134] Som SK, Datta A. Thermodynamic irreversibilities and exergy balance in combustion processes. Prog Energy Combust Sci 2008;34:351–76. doi:10.1016/j.pecs.2007.09.001.

[135] Wang L, Karimi N, Paul MC. Gas-phase transport and entropy generation during transient combustion of single biomass particle in varying oxygen and nitrogen atmospheres. Int J Hydrogen Energy 2018;43:8506–23. doi:10.1016/j.ijhydene.2018.03.074.

[136] Wang L, Karimi N, Sutardi T, Paul MC. Numerical modelling of unsteady transport and entropy generation in oxy-combustion of single coal particles with varying flow velocities and oxygen concentrations. Appl Therm Eng 2018;144:147–64. doi:10.1016/j.applthermaleng.2018.08.040.

[137] Li ZW, Chou SK, Shu C, Yang WM. Entropy generation during microcombustion. J Appl Phys 2005;97:084914. doi:10.1063/1.1876573.

[138] Jejurkar SY, Mishra DP. Numerical analysis of entropy generation in an annular microcombustor using multistep kinetics. Appl Therm Eng 2013;52:394–401. doi:10.1016/j.applthermaleng.2012.12.021.

[139] Rana U, Chakraborty S, Som SK. Thermodynamics of premixed combustion in a heat recirculating micro combustor. Energy 2014;68:510–8. doi:10.1016/j.energy.2014.02.070.

[140] Rana U, Chakraborty S, Som SK. Prediction of flame speed and exergy analysis of premixed flame in a heat recirculating cylindrical micro combustor. Energy 2017;126:658–70. doi:10.1016/j.energy.2017.03.063.

[141] Jiang D, Yang W, Teng J. Entropy generation analysis of fuel lean premixed CO/H2/air flames. Int J Hydrogen Energy 2015;40:5210–20. doi:10.1016/j.ijhydene.2015.02.082.

[142] Wenming Y, Dongyue J, Kenny CKY, Dan Z, Jianfeng P. Combustion process and entropy generation in a novel microcombustor with a block insert. Chem Eng J 2015;274:231–7. doi:10.1016/j.cej.2015.04.034.

[143] Jiaqiang E, Zuo W, Liu X, Peng Q, Deng Y, Zhu H. Effects of inlet pressure on wall temperature and exergy efficiency of the micro-cylindrical combustor with a step. Appl Energy 2016;175:337–45. doi:10.1016/j.apenergy.2016.05.039.

[144] Wang W, Liu J, Zuo Z, Yang W. Entropy generation analysis of unsteady premixed methane/air flames

in a narrow channel. Appl Therm Eng 2017;126:929–38. doi:10.1016/j.applthermaleng.2017.07.176.

[145] Nadimi E, Jafarmadar S. The numerical study of the energy and exergy efficiencies of the micro-combustor by the internal micro-fin for thermophotovoltaic systems. J Clean Prod 2019;235:394–403. doi:10.1016/J.JCLEPRO.2019.06.303.

[146] Ni S, Zhao D, Sun Y, Jiaqiang E. Numerical and entropy studies of hydrogen-fuelled micro-combustors with different geometric shaped ribs. Int J Hydrogen Energy 2019;44:7692–705. doi:10.1016/J.IJHYDENE.2019.01.136.

[147] Zuo W, Zhang Y, Li J, Li Q, He Z. A modified micro reactor fueled with hydrogen for reducing entropy generation. Int J Hydrogen Energy 2019;44:27984–94. doi:10.1016/J.IJHYDENE.2019.09.009.

[148] Hunt G, Karimi N, Torabi M. Two-dimensional analytical investigation of coupled heat and mass transfer and entropy generation in a porous, catalytic microreactor. Int J Heat Mass Transf 2018;119:372–91. doi:10.1016/j.ijheatmasstransfer.2017.11.118.

[149] Karimi N, Agbo D, Talat Khan A, Younger PL. On the effects of exothermicity and endothermicity upon the temperature fields in a partially-filled porous channel. Int J Therm Sci 2015;96:128–48. doi:10.1016/J.IJTHERMALSCI.2015.05.002.

[150] Alizadeh R, Karimi N, Nourbakhsh A. Effects of radiation and magnetic field on mixed convection stagnation-point flow over a cylinder in a porous medium under local thermal non-equilibrium. J Therm Anal Calorim 2019:1–21. doi:10.1007/s10973-019-08415-1.

[151] Gomari SR, Alizadeh R, Alizadeh A, Karimi N. Generation of entropy during forced convection of heat in nanofluid stagnation-point flows over a cylinder embedded in porous media. Numer Heat Transf Part A Appl 2019;75:647–73. doi:10.1080/10407782.2019.1608774.

[152] Alizadeh R, Karimi N, Mehdizadeh A, Nourbakhsh A. Analysis of transport from cylindrical surfaces subject to catalytic reactions and non-uniform impinging flows in porous media. J Therm Anal Calorim 2019;138:659–78. doi:10.1007/s10973-019-08120-z.

[153] Hunt G, Karimi N, Yadollahi B, Torabi M. The effects of exothermic catalytic reactions upon combined transport of heat and mass in porous microreactors. Int J Heat Mass Transf 2019;134:1227–49. doi:10.1016/j.ijheatmasstransfer.2019.02.015.

[154] Saeed A, Karimi N, Hunt G, Torabi M. On the influences of surface heat release and thermal radiation upon transport in catalytic porous microreactors—A novel porous-solid interface model. Chem Eng Process - Process Intensif 2019;143:107602. doi:10.1016/J.CEP.2019.107602.

[155] Saeed A, Karimi N, Hunt G, Torabi M, Mehdizadeh A. Double-diffusive transport and thermodynamic analysis of a magnetic microreactor with non-Newtonian biofuel flow. J Therm Anal Calorim 2019:1–25. doi:10.1007/s10973-019-08629-3.

Table 1. Summary of the existing studies on entropy generation rate in microchannels.

Articles	System configuration	System or sub-system modeling	Method of analysis	Single-phase or multiphase
Naphon [7]	Concentric micro-fin tube heat exchanger	System modeling	Experimental and analytical	Single-phase flow
Elliott et al. [26]	Asymmetric porous microchannel with thick walls	Sub-system modeling	Analytical	Single-phase flow
Hunt et al. [27]	Asymmetric partially porous microchannel with thick walls	Sub-system modeling	Analytical	Single-phase flow
Li et al. [32]	Microchannels with triangular cavities and rectangular ribs	Sub-system modeling	Numerical	Single-phase flow
Zhai et al. [64]	Microchannels with various cavities and ribs	Sub-system modeling	Numerical	Single-phase flow
Torabi and Peterson [63]	Porous microchannel with thick walls, and velocity slip and temperature jump	Sub-system modeling	Analytical	Single-phase flow
Türkakar and Okutucu-Özyurt [65]	Rectangular microchannel	System modeling	Analytical/Numerical	Multiphase flow
Türkakar et al. [47]	Air cooled aluminum condenser with parallel flow microchannels	System modeling	Analytical/Numerical	Multiphase flow
Abdous et al. [66]	Micro-fin tube-in-tube heat exchangers	System modeling	Analytical	Multiphase flow

Table 2. Summary of the existing studies on entropy generation rate in microcombustors and microreactors.

Articles	Microcombustor/microreactor configuration	Mode of combustion/reaction	Fuel	Methodology and Major findings
Li et al. [137]	Axisymmetric and annular	Premixed	H_2	Analytical- Stoichiometric operation leads to the lowest second law efficiency.
Jejurkar and Mishra [33]	Axisymmetric and annular	Premixed	H_2	Numerical- optimal exergetic behavior is achieved at the wall therm conductivity of 0.1-1.75 W/m K.
Jejurkar and Mishra [138]	Axisymmetric and annular	Premixed	H_2	Numerical- Multistep chemistry was implemented and it was show that chemical irreversibility is heavily affected by low-temperatur
Jiang et al. [24]	Axisymmetric and annular with heat recuperator	Premixed	H_2	Numerical- increasing the flow velocity of the reactants intensifies irreversibility.
Jiang et al. [25]	Planar with baffles	Premixed	H_2	Numerical- Second law efficiency decrease for higher baffle heights
Rana et al. [140][139]	Thick-wall-axisymmetric	Premixed	Any gaseous fuel	Analytical- exergy loss at the outer wall is between 5-7% of the infl exergy and, heat recirculation and combustion account for the dest around 40-45% of the inflow exergy.
Jiang et al. [141]	Circular cylinder microchannel	Premixed	$CO+H_2$	Numerical- For low CO concentrations in the reactants, $OH+H_2O=H$ the most irreversible reaction. For high CO concentrations, the rela contribution of $CO+OH=CO_2+H$ increases.
Jiaqiang et al. [143]	Cylindrical with a step	Premixed	H_2	Numerical- Inlet pressure has significant effects on the entropy ger rate.
Wang et al. [144]	Planar	Premixed	CH_4+H_2	Numerical- at low H_2 concentrations, $CH_3+O=CH_2O+H$ dominates th chemical irreversibility. Further addition of hydrogen magnifies th $H+O_2+M=H_2O+M$.
Nadimi and Jafarmadar [145], Zuo et al. [147], Ni et al. [146]	3D complex structures	Premixed	H_2	The shape and material of the solid body of micro-combustor can significantly affect the rate of entropy generation rate.
Elliot et al. [26], Saeed et al. [155], Guthrie et al. [30]	Planar-non-axisymmetric thick wall	Homogeneous chemical reactions	N/A	One-dimensional analytical - The wall thickness was found to be in Mass transfer strongly affects the total irreversibility of the system
Hunt et al. [75]	Planar- non-axisymmetric thick wall	Homogeneous chemical reactions	N/A	Two-dimensional analytical - The wall thickness was found to be ir Mass transfer strongly affects the total irreversibility of the system
Govone et al. [106]	Planar- non-axisymmetric thick wall	Heterogenous catalytic reactions	N/A	One-dimensional analytical -Mass transfer process in general and t diffusion of mass in particular were found to be essential in genera entropy.
Hunt et al. [149][150], Saeed et al. [154]	Planar- non-axisymmetric thick wall	Heterogenous catalytic reactions	N/A	Two-dimensional analytical -Mass transfer process in general and t diffusion of mass in particular were found to be essential in genera entropy.

Table 3. Summary of mathematical equations for entropy generation rate in micro energy systems.

Equation	No.	Equation
$dsdt=msin-msout+QT+Sgen,tot$	(22)	$-\partial p\partial x+\mu eff\partial 2uf1\partial y2-\mu f\kappa uf1=0 \quad h1\leq y<h2$
$Sgen,tot=segmentmasa,out-sa,in+mrsr,out-sr,in$	(24)	$-\partial p\partial x+\mu f\partial 2uf2\partial y2=0 \quad h2\leq y\leq h3$
$\rho cpu\partial T\partial x=k\partial 2T\partial y2+\mu dudy2$	(25)	$k1ddydT1dy+q1=0 \quad 0<y\leq h1$
$S'''=kT2\partial T\partial x2+\partial T\partial y2+\mu T\partial u\partial y2$	(27)	$\rho cpuf1\partial Tf1\partial x=kef\partial 2Tf1\partial y2+hsfasfTs-Tf1+sf \quad h1\leq y<h2$
$S'''=kmT2\partial T\partial x2+\partial T\partial y2+\mu\kappa Tu2+\mu T\partial u\partial y2$	(28)	$0=kes\partial 2Ts\partial y2-hsfasfTs-Tf1+ss \quad h1\leq y<h2$
$Sf'''=kefTf2\partial Tf\partial x2+\partial Tf\partial y2+hsfasfTs-TfTf+\mu\kappa Tfuf2+\mu Tf\partial uf\partial y2$	(29a)	$\rho cpuf2\partial Tf2\partial x=kf\partial 2Tf2\partial y2+sf \quad h2\leq y\leq h3$
$Ss'''=kesTs2\partial Ts\partial x2+\partial Ts\partial y2-hsfasfTs-TfTf$	(29b)	$k2ddydT2dy+q2=0 \quad h3<y\leq h4$
$Sgen,a=masa,out-sa,in=macp,alnTa,outTa,in-RlnPa,outPa,in$	(30)	$\boldsymbol{Si=Qi\ Ti,s-\ Ti,f}$
$ds=diTr-vdPrTr=diTr-dPr\rho Tr$	(32)	$di=Tds-Pdvsp+i=1n\mu idYi,$
$Sgen,\Delta P=mrsegment\Delta PrTr\rho r-masegment RlnPa,outPa,in$	(34)	$TDsDt=DiDt-P\rho 2D\rho Dt-i=1n\mu iDYiDt.$
$Sgen,ht=segmentmacp,alnTa,outTa,in+mrsout-sin-mr\Delta PrTr\rho r$	(36)	$\rho DsDt=1T\nabla.kmix\nabla T-1T\nabla.i=1nhiJi+\phi T+1Ti=1n\mu i\nabla.Ji-1Ti=1n\mu iri.$
$\rho DsDt=\nabla.qT+1Ti=1n\mu iJi+1T2kmix\nabla T2-1T2i=1nhi.Ji.\nabla T+\phi T-1Ti=1n\mu iri+1Ti=1nJi.1T\mu i\nabla T-\nabla\mu i$	(38)	$sgen'''diff=i=1n(\rho RiDim)\nabla Yi.\nabla XiXi+i=1nRiDTi[\nabla TT\nabla XiXi]$

$sR=\nabla.qT+1Ti=1n\mu iJi$	(39a)	$sgen'''vis=\phi T$
$sgen'''total=1T2kmix\nabla T2-1T2i=1n\hbar iJi\nabla T+\phi T-1Ti=1n\mu iri+1Ti=1nJi.[1T\mu i\nabla T-\nabla\mu i]$	(39b)	$sgen'''rad,s=1TR,s\alpha s4\pi Ib,s-Gs-1Ts\alpha s4\pi Ib,s-Gs$
$sgen'''r=-1Ti=1n\mu iri$	(41a)	$sgen'''rad,g=1TR,g\alpha g4\pi Ib,g-Gg-1Tg\alpha g4\pi Ib,g-Gg$
$sgen'''cond=1T2kmix\nabla T2$	(41b)	$sgen'''total=sgen'''r+sgen'''cond+sgen'''diff+sgen'''vis+sgen'''rad,s+sge$

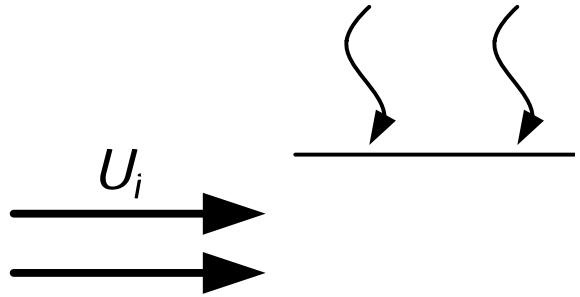

Fig. 1. Schematic of a simple rectangular duct

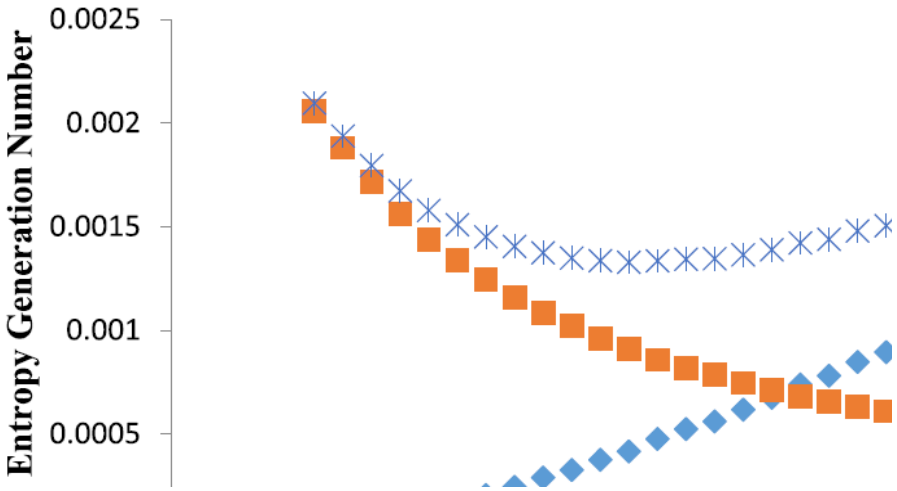

Fig. 2. Optimization of total entropy generation number versus mass flow rate of air in a microchannel condenser [47].

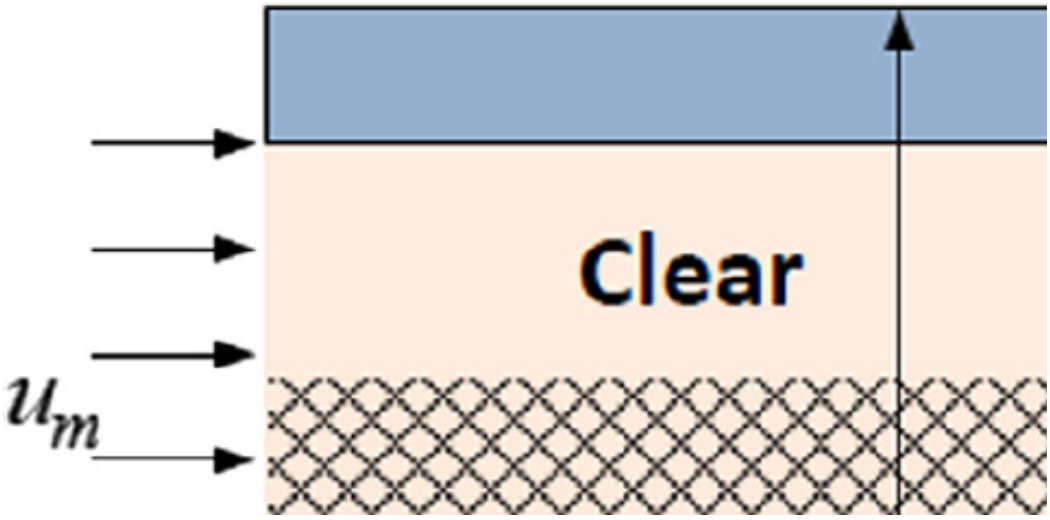

Fig. 3. Partially filled porous microchannel with thick walls [27].

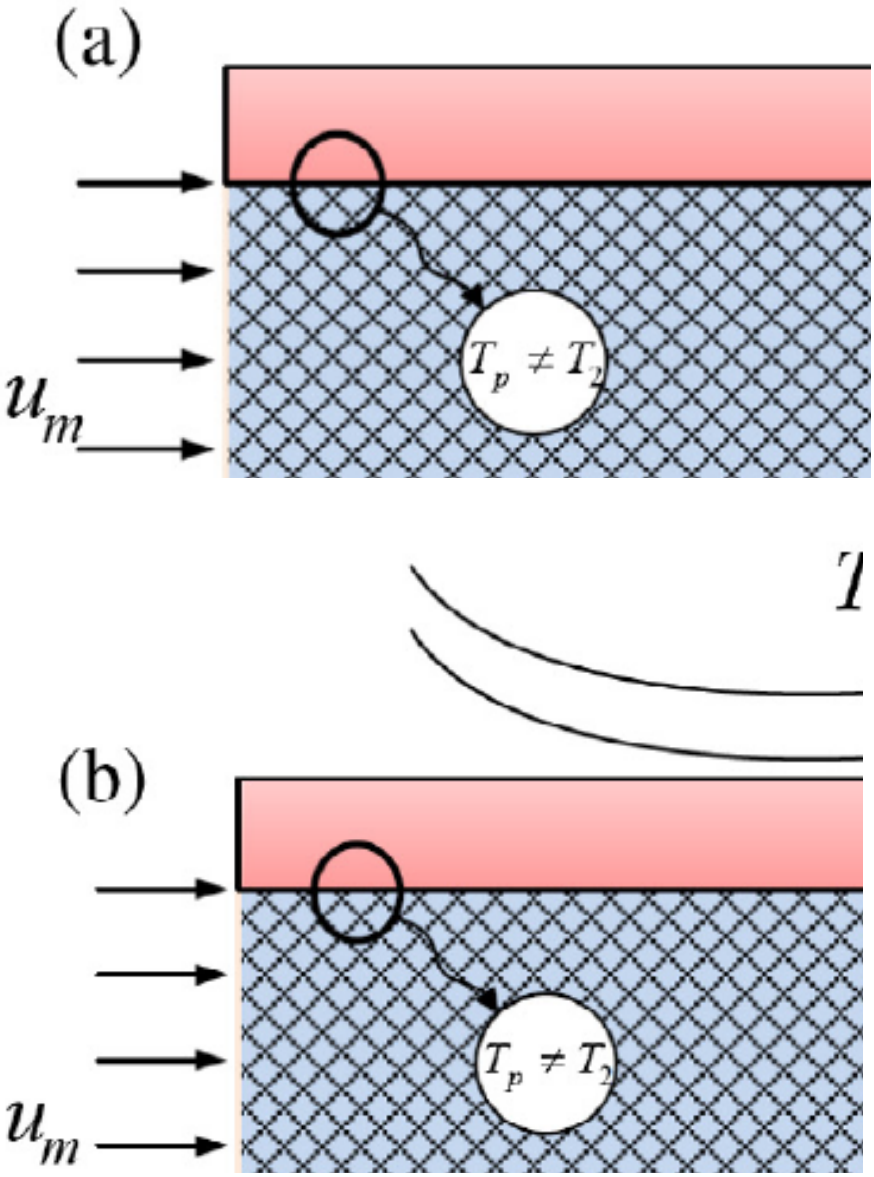

Fig. 4. Configuration and boundary conditions of two microchannels filled with a porous material considering temperature jump between walls and fluid [78].

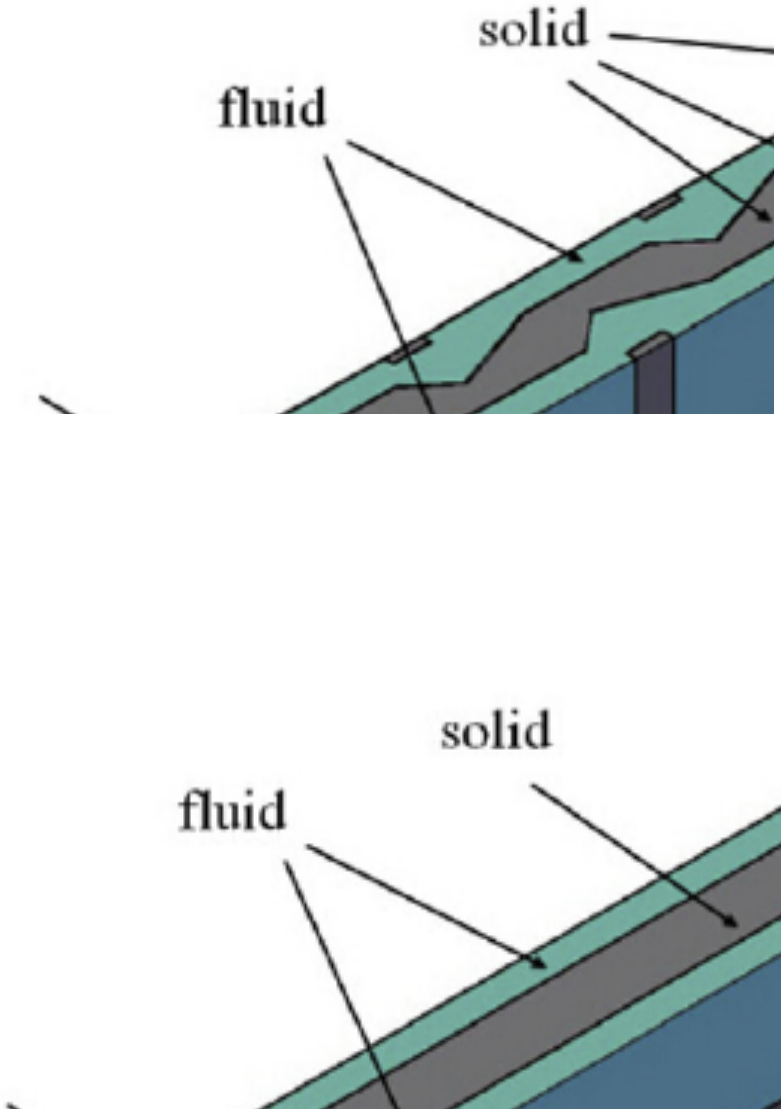

Fig. 5. Schematic diagrams of TC–RR and CR microchannels [32].

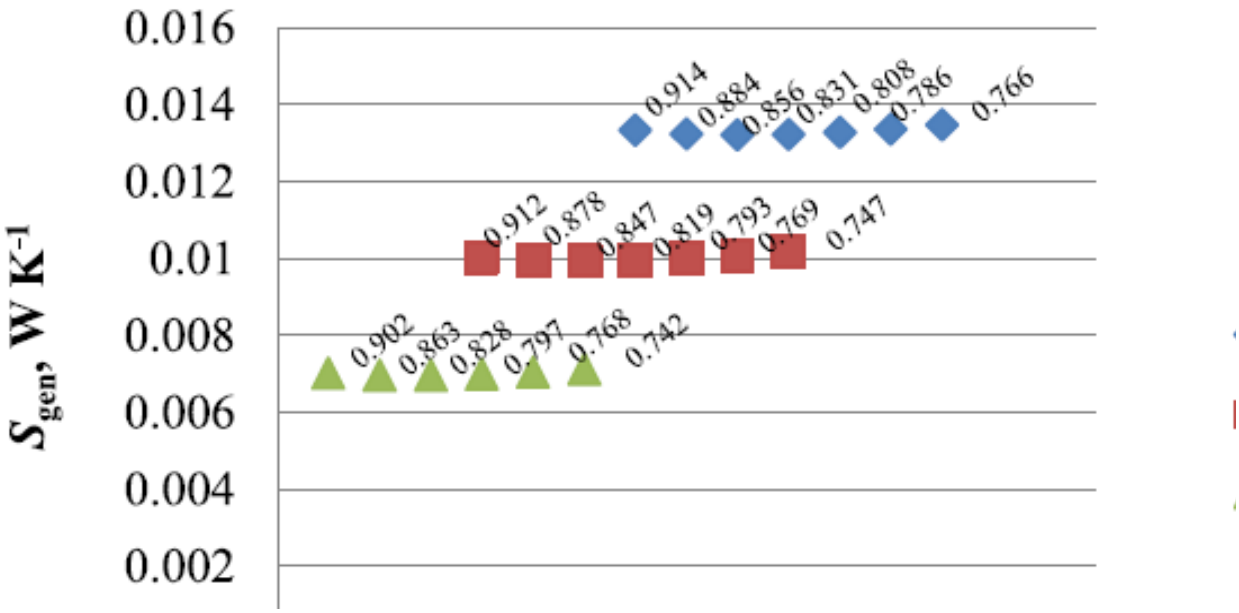

Fig. 6. Variation of entropy generation rate versus mass flow rate for different heat fluxes in an evaporator [65].

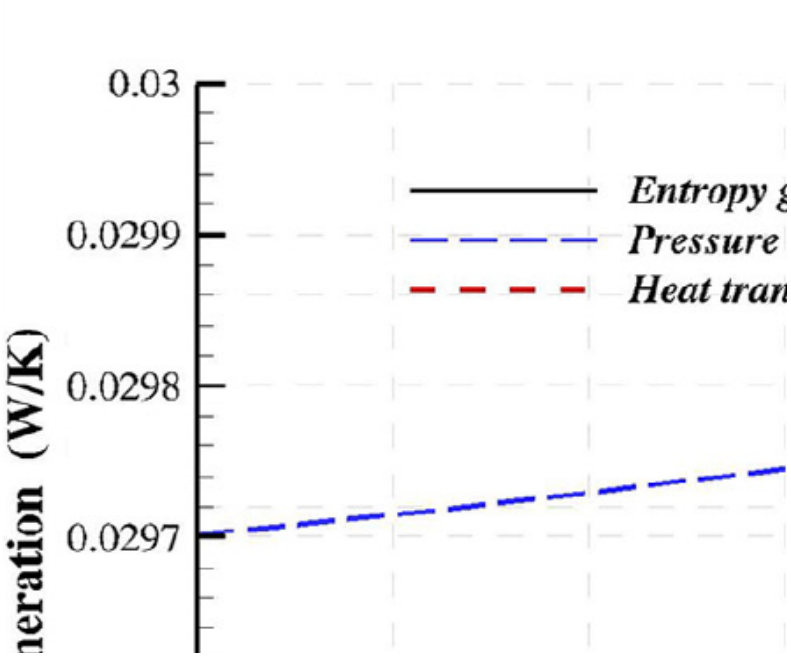

Fig. 7. Effects of number of micro-fins on heat transfer and pressure drop contributions of entropy generation rate in tube-in-tube heat exchangers [66].

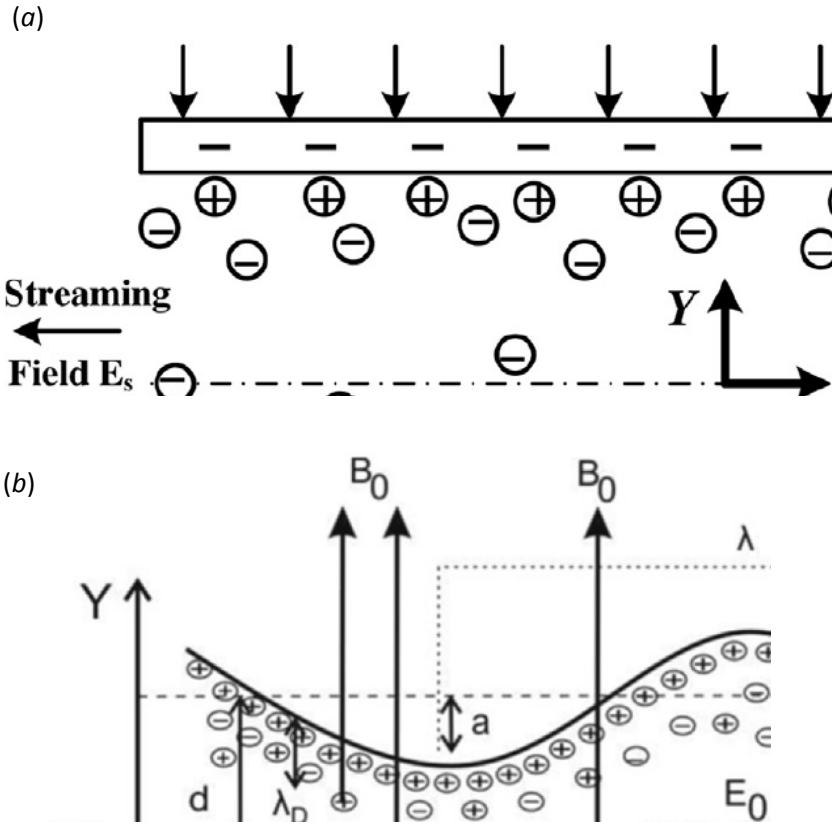

Fig. 8. Schematic of two types of microchannels accommodating fluid flow and electromagnetic under entropy generation rate investigation: (a) parallel plate microchannel by Zhao et. al [95], and (b) microchannel under uniform peristaltic wave [96].

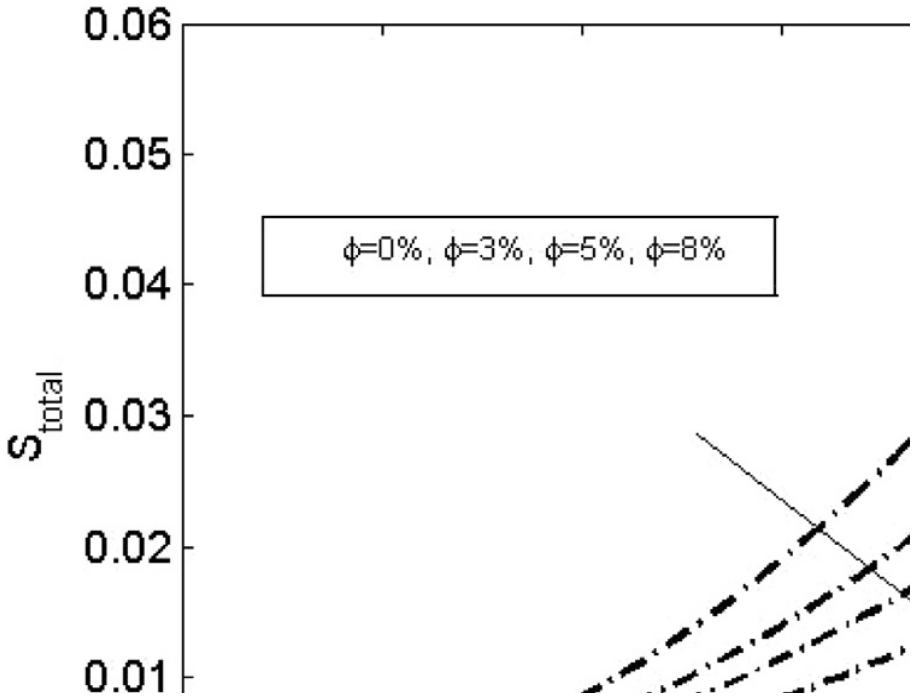

Fig. 9. Sample results for simulation of nanofluids in microchannel with streaming potential effects: Effects of nanoparticles concentration and Brinkman number on the total entropy generation rate [95].

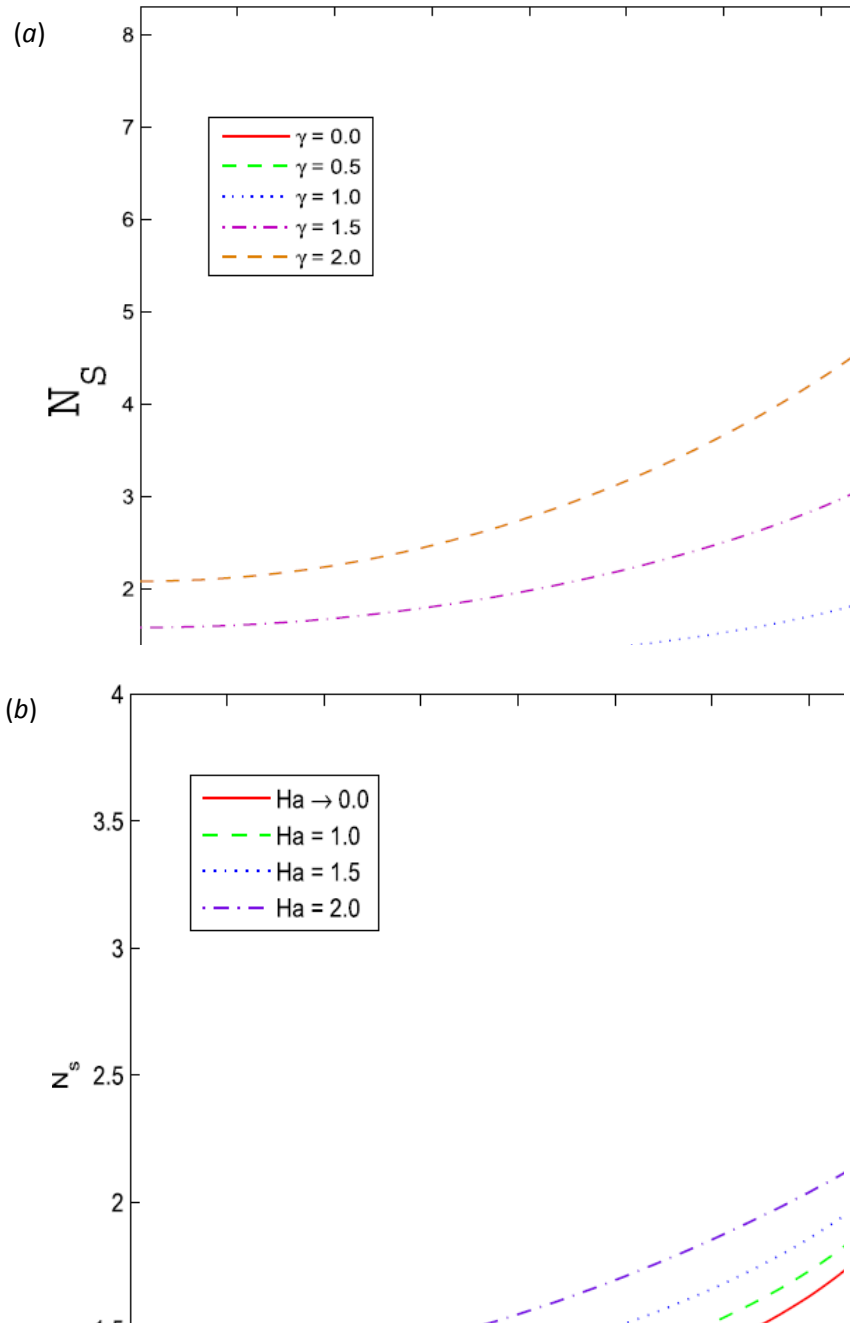

Fig. 10. Local entropy generation rate variation along a microchannel for different values of (a) Joule heating parameter, and (b) Hartmann number [96].

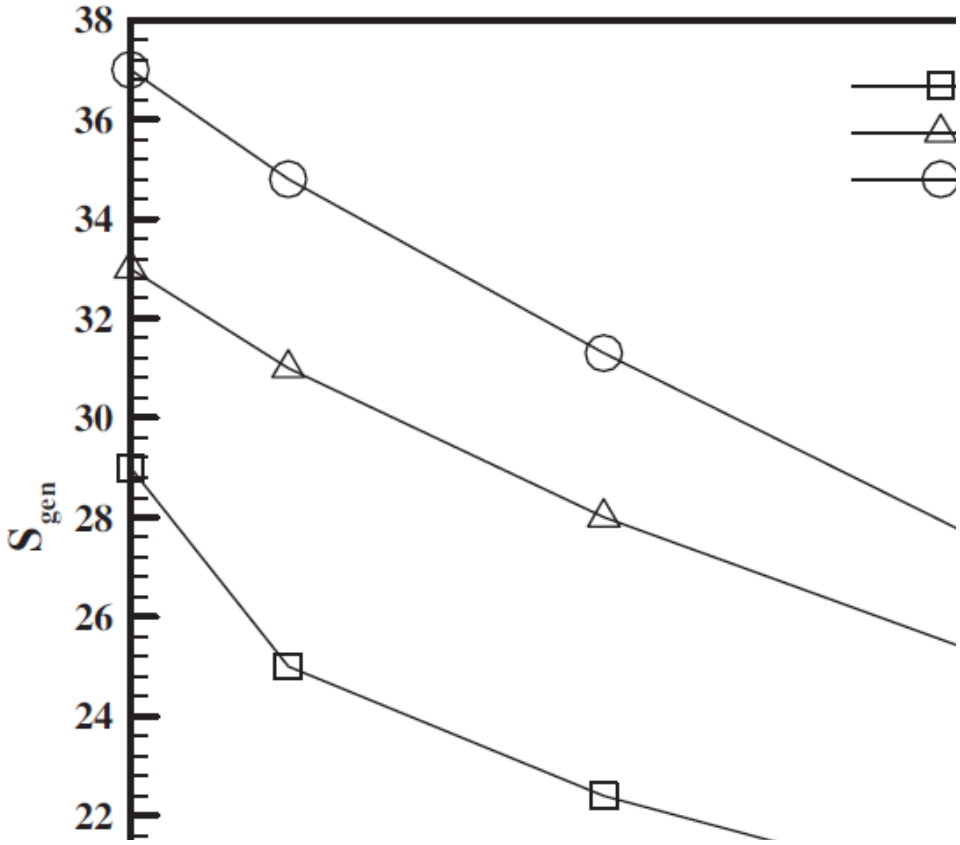

Fig. 11. Variation of the total entropy generation rate with aspect ratio and Reynolds number resulted from numerical simulation of nanofluid flow through a three-dimensional microchannel with magnetic effects [110].

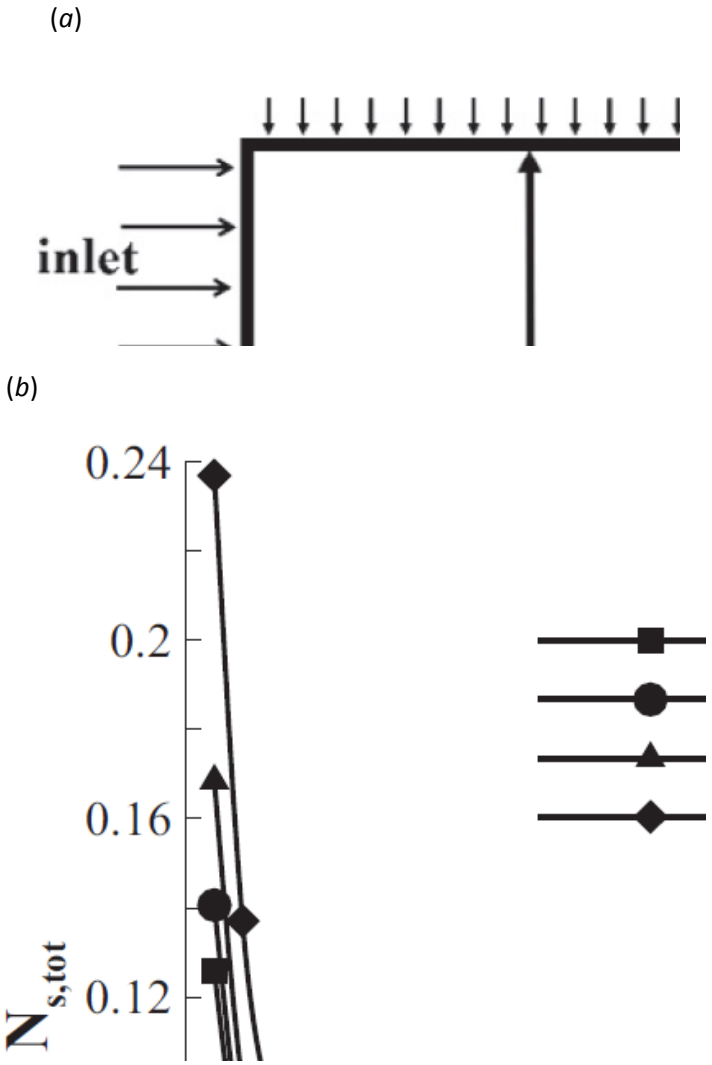

Fig. 12. (a) Schematic of annuli heat exchanger with nanofluid flow considered for entropy generation rate investigation, and (b) sample entropy generation rate optimization for different Reynolds numbers [120].

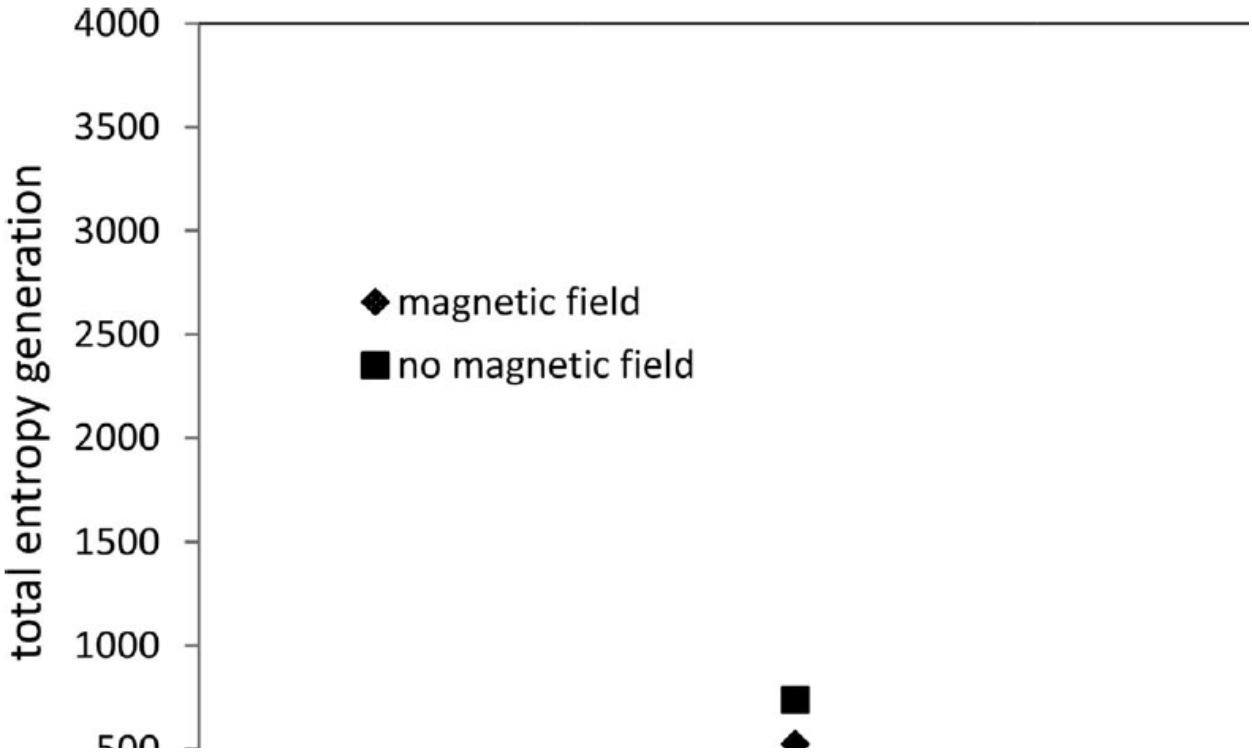

Fig. 13. Effects of magnetic field and Rayleigh number on the total entropy generation rate within a nanofluid filled cavity [121].

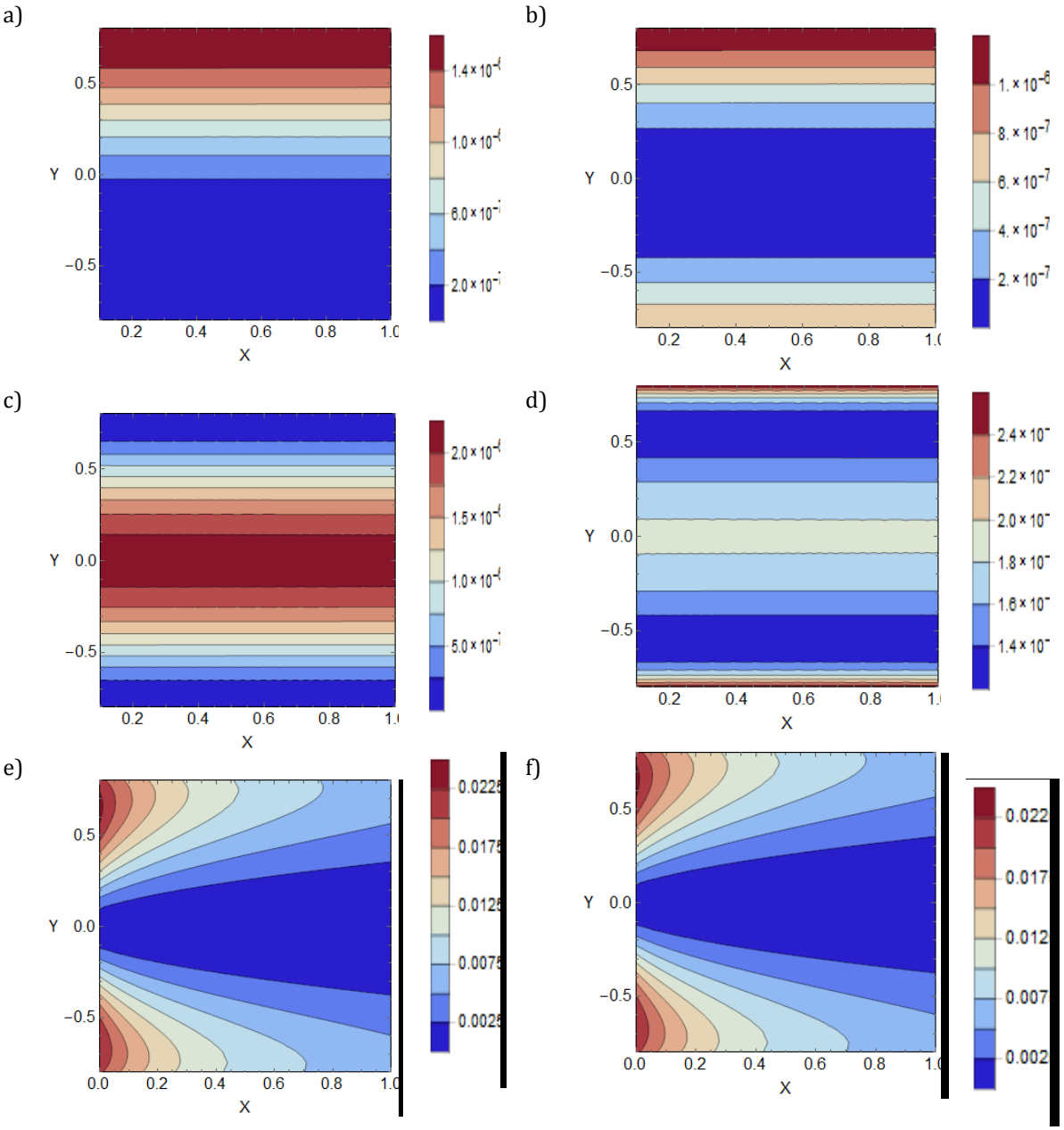

Fig. 14. Contours of dimensionless entropy inside a porous, thermochemical catalytic microreactor a) thermal entropy in porous solid phase , b) thermal entropy in the fluid phase, c) thermal entropy generation rate due to heat exchange between fluid and sloid phases inside the porous medium, d) viscous entropy generation rate, e) mass transfer entropy generation rate and f) total entropy generation rate [148].